Dear Editor,

Thanks for your help and the two reviewers' kind suggestions. Accordingly, we have finished the revision of the manuscript, including (1) instrumental and field instruction in detail, (2) explanation on greater fluctuation of spring ozone at Zhonshan Station. We also analyzed the STT by CAM-Chem model but not added this part into manuscript, which can be found in the Reply to reviewers.

The new version is now ready for your consideration, we think. Please contact us if there is still flaws.

Best Regards,

Minghu
on behalf of all authors

Reply for Anonymous Referee #1

The manuscript is within the scope of ESSD. It presents scientifically significant material based on surface ozone measurements at three Antarctic stations. Of especial importance are data of measurements at Dome A, the highest Antarctic plateau (4000 m above sea level), which is one of the remotest areas on earth. The analysis of the data is reasonable and reliable, the data is unique. The authors should consider the following comments prior to publication.

General comments

1. I would appreciate it if the authors could please introduce more about the details of instruments and the measurements.

Reply： The detailed information of these instrument and observation introduction has been added in Section 2.1. Please find it in the Tracking version of the manuscript.

2. Because the results of trajectory clustering analysis are important in the discussion, there should be more description of trajectory clustering method.

Reply： The introduction of the trajectory cluster was added in Section 2.3, as bellow.

"The air mass trajectories were assigned to distinct clusters according to their moving speed and direction using a k-means clustering algorithm (Wong, 1979). Concerning with this study focused on transport pathway of O_3, the clustering result with the smallest number was selected as done by Wang et al., (2014). It was found three clusters performance best to represented the meteorological characteristics of the transport pathways at DA. This number was then selected as the expected number of air mass trajectory clusters. A more detailed clustering procedure using the k-means algorithm can be found in Wang et al. (2014)."

3. L64-70. The specific chemical reaction process of nitrate aerosol photodegradation on snow pack should be increased. It is necessary to clarify the effect of NOx released by photodegradation on O_3 emission from snow pack if it is possible.

Reply： According to your suggestion, the photochemical reaction process of snow surface is supplemented in Section 1. These explanation and correction have been added in the context (line 67-69).

L67-L69: "As the solar irradiance and the nitrate aerosol concentration increase, the emission of NO_X will increase through the photodenitrification process of the summer snowpack (e.g. $NO^{3-}+hv \rightarrow NO^{2}+O^{-}$; $O^{-}+H^{+} \rightarrow OH$; Honrath et al., 2000; Warneck et al., 1989)."

4. In Section 3.3, the author's statement is too simple and arbitrary. The standard deviation of the average daily concentration in Zhongshan station was significantly higher than that in the other two inland stations. L259-L264 completely said that every solar chemical reaction had little effect on the concentration variation characteristics of the three stations, which was not rigorous. This paper focuses on the influence of daily photochemical reaction on the concentration variation characteristics of Dome A, and the difference of average daily concentration fluctuation between coastal stations and inland stations also needs to be

discussed briefly. For example, coastal stations are easily affected by halogen gas mass in summer, and ODE (Ozone Depletion Event) is triggered (A.E. Jones et al., 2009), which has obvious impact on the fluctuation of average daily concentration in summer. Section 3.3 needs to add relevant references to support the author's statement.

Reply: Thanks for your suggestion. As a coastal station, the average daily concentration fluctuation in Zhongshan station was obviously different with the two inland stations, which can be attributed into their background climates. In Spring, ODEs occur frequently at Zhongshan Station. And this phenomenon always accompanies with abrupt weather transit from continental dominant to oceanic dominant, in other words, the BrO brought by northerly wind from sea ice area could leaded to serious ozone depletion (Wang et al., 2011; Ye et al., 2018). Whereas at inland stations like DA and SP, there were rarely ODEs.

These explanation and correction have been added in the context.

5. In Section 4, the influence of STT on OEE is discussed by STEFLUX. It is also mentioned that STT can be judged by atmospheric chemical model (such as GFDL-AM3 and CAM-CHEM). Can author try to use CAM-CHEM Model to analyze the STT events in Dome A and compare the results with the OEE. At the same time, results of the two methods may be compared if it is possible.

Reply： Thank you for your suggestion. Starting to analyze the results of CAM-CHEM model after receiving this reply. But the results reflect an interesting phenomenon.

During the whole polar night, the results of CAM-CHEM model show that STT occur frequently over DA (Figure 1). However, the frequency of OEEs is lower than that of STT events. During the whole polar night, much times of STT promoted the increase of near surface ozone concentration of DA. However, on the one hand, the occurrence of OEE during the polar night is affected by STT. On the other hand, it may be related to the specific meteorological conditions. Based on the statistics of the meteorological elements of OEE and NOEE during the polar night (Table 1), the average wind speed was low and the average height of the planet boundary layer (PBL) was 66.46m. Moreover, the lower mean potential vorticity at 550 Hpa implies a stronger vertical downward transport process. The lower wind speed makes the high concentration ozone grow rapidly near the ground.

Compared with the analysis results of STEFLUX tool and CAM-CHEM model, the STEFLUX tool has a good selection for “deep” STT process. But the results show that “deep” STT process has little effect on OEE. However, the model results better reflect the frequent occurrence of STT over DA during the polar night, which is an important reason for the continuous accumulation of near surface ozone concentration during the polar night. However, the low frequency of OEE makes it difficult to establish a direct relationship with the model results. Under the frequent STT, the stable boundary layer condition with low wind speed near the ground is helpful to the occurrence of OEE.

Interestingly, on May 31, both the pattern results and STEFLUX results showed a strong STT, and OEE occurred on that day. The combination of the two methods makes us have more interesting findings. We hope to analyze such events in the future based on the meteorological data of DA and relevant model methods.

These findings is not the main purpose of the paper, we want to conduct a new detailed study on the comparison of the two methods in the future. However, if you insist to add this part, it can be done in the next modification.

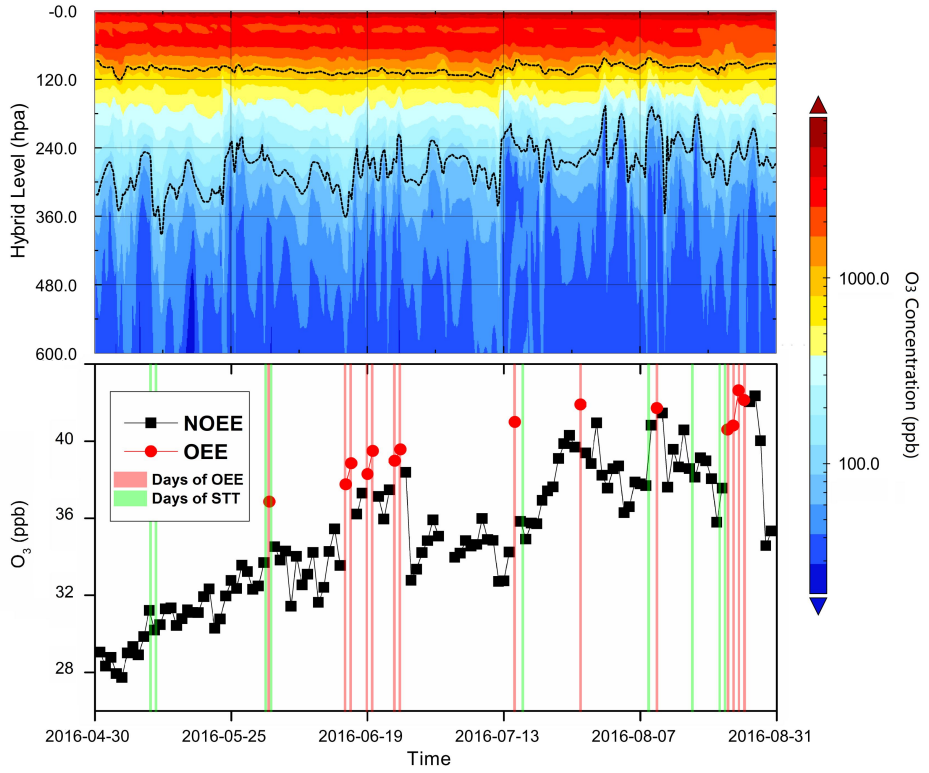

Figure 1 The vertical distribution of ozone concentration over DA was calculated by CAM-CHEM model. During the polar night, the fluctuation of ozone concentration, the distribution of OEE and "deep" STT.

Table 1 The mean wind speed, air temperature, PBL and 550Hpa potential vorticity of OEEs and NOEEs during the polar night.

Days	Wind Speed (m/s)	Temperature (℃)	PBL (m)	550Hpa PV
OEEs	2.77	-33.07	66.46	-3.47
NOEEs	3.13	-35.66	32.29	-2.55

6. Table 1 is not necessary, I suggest to delete it or move it to supplementary.

Reply： According to your suggestion, the original Table 1 was deleted. The comparison of instrument parameters of the three stations is supplemented to replace the contents in Table 1.

7. Fig. or Figure, please use the unified one in the whole paper.

Reply： It has been done.

Specific comments

1. Line 22, what is DA.

Reply： It has been modified.

2. Line 232, only “in this part"? Sept—Sep?

Reply： It has been modified.

3. Line 217-220, “concentration, molar ratio, mixting ratio", please be consistent with each others.

Reply： The three words were unified as **concentration** in the full text.

4. Line 282, from the results above, “it can be seen that" SP was characterized....

Reply： It has been modified.

5. Line 301, the wind of DA were “predominantly" from north and west. Prevalent may be better.

Reply： It has been modified.

6. Line 317, have — has.

Reply： It has been modified.

7. Line 361, As the station name has been abbraviatted, such as Amundsen-Scott —SP, all station names should be checked and properly used.

Reply： It has been modified and the station names has been checked.

8. Line 375-376, the last sentence should be rewrite or removed.

Reply： The sentence has been removed.

9. I would suggest improving the readability of the label in Figure 4 if it is possible. It seems to not clear on my copy.

Reply： The figure in the PDF file were compressed, and the clear and non-destructive image was replaced.

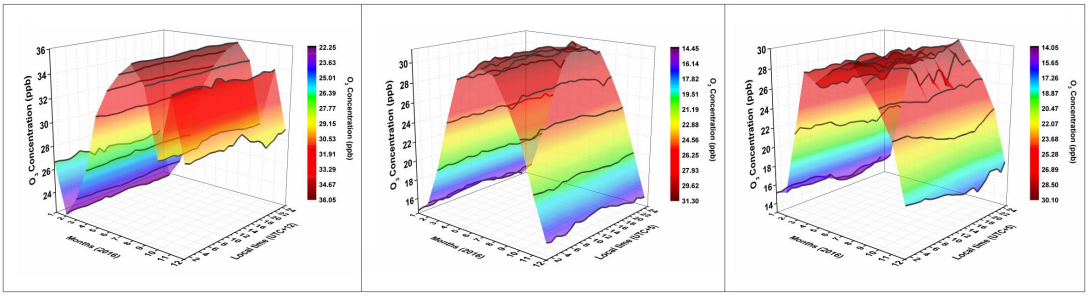

10. Figure 5, Standard deviations of mean diurnal variation in near-surface....

Reply： It has been modified.

11. Figure 8, what are the error bars.

Reply： Error bars are the standard deviation of the same cluster. The explanation has been added in the caption.

12. Figure 11, δ should be △?

Reply： It has been modified.

Reply for Anonymous Referee #2

Ozone is a major short-lived air pollutant when presents near ground, besides, it is a greenhouse gas that exerts direct influence on radiative forcing. The understanding of the variability and source of ground ozone in Antarctica remained limited, particularly in the inner Antarctica. In this paper, authors reported year-round observation of ozone in Dome A, the highest plateau in the Antarctica, they also complied observation data from South Pole and a costal site to make comparison. They revealed the occurrence of ozone enhancement events (OEEs) at Dome A and analyzed the possible sources and transport that contribute to the OEEs. The technical quality of the paper, including its observation and data analysis, is generally good. I have two major concerns on the manuscript.

General comments

1. The ESSD journal concentrates on datasets and the related process of data production. The current version of the paper did provide valuable time series of year-round ozone observation at Dome A, but it reads more like a research paper and author performed comprehensive diagnoses on the OEEs. I would leave the decision on the suitability of the paper for the journal to the editor.

Reply： Thank you for your advice. In this article, we did not only introduced the ozone data of DA, but also hoped to show some different characteristics with other Antarctic stations. It can provide more information to the readership.

To highlight the importance of the data and the reliability of the observation, detailed introduction on the three instruments and field plan were added in Section 2.1.

2. Authors focused on ozone variability and OEEs at Dome A, they also included data from South Pole and a coastal site of Zhongshan Station and revealed different patterns of ozone variabilities in the three sites. However, in section 4, authors only analyzed the OEEs at Dome A site. The question is what's the purpose of including data from other two sites? Section 3 and 4 are not closely linked and I suggest authors to rethink the aims of the paper to stick to the main topic, e.g., differences in variabilities of ozone at three sites and possible reasons, or alternatively, the finding of strong OEEs at Dome A and its possible underlying mechanisms.

Reply： Thank you for your comments. As you said, section 3 introduced the surface ozone characteristics of DA, SP and ZS, section 4 introduced OEEs only in DA but not SP and ZS. That is because we found only at DA, there were OEEs in winter. The other two, only have summer OEEs. And several studies have carried out on the causes of summer OEEs, such as Cristofanelli et al. (2018) and Legrand et al., (2016). They suggested continental transport was the key reason. Thus we wanted to focus on the unclear one, which was the winter OEEs.

In Section 4.1, the first paragraph introduced the method, the second paragraph introduced the general OEEs results of the three stations, the third paragraph introduced the differences of OEEs among the stations and highlighted the speciality of DA (winter OEEs). Then, the

fourth paragraph explained the findings of summer OEEs by previous studies. This logics was aimed to bring up the 4.2 and 4.3, which was the discussion on DA OEEs.

Anyway, if you think it is not suitable, we can delete this part and focus on general comparison among the three stations.

3. Figure 8 and 9 can be combined into one figure and the layouts of the figure should be re-designed to make it neat and clear.

Reply： The figures has been merged.

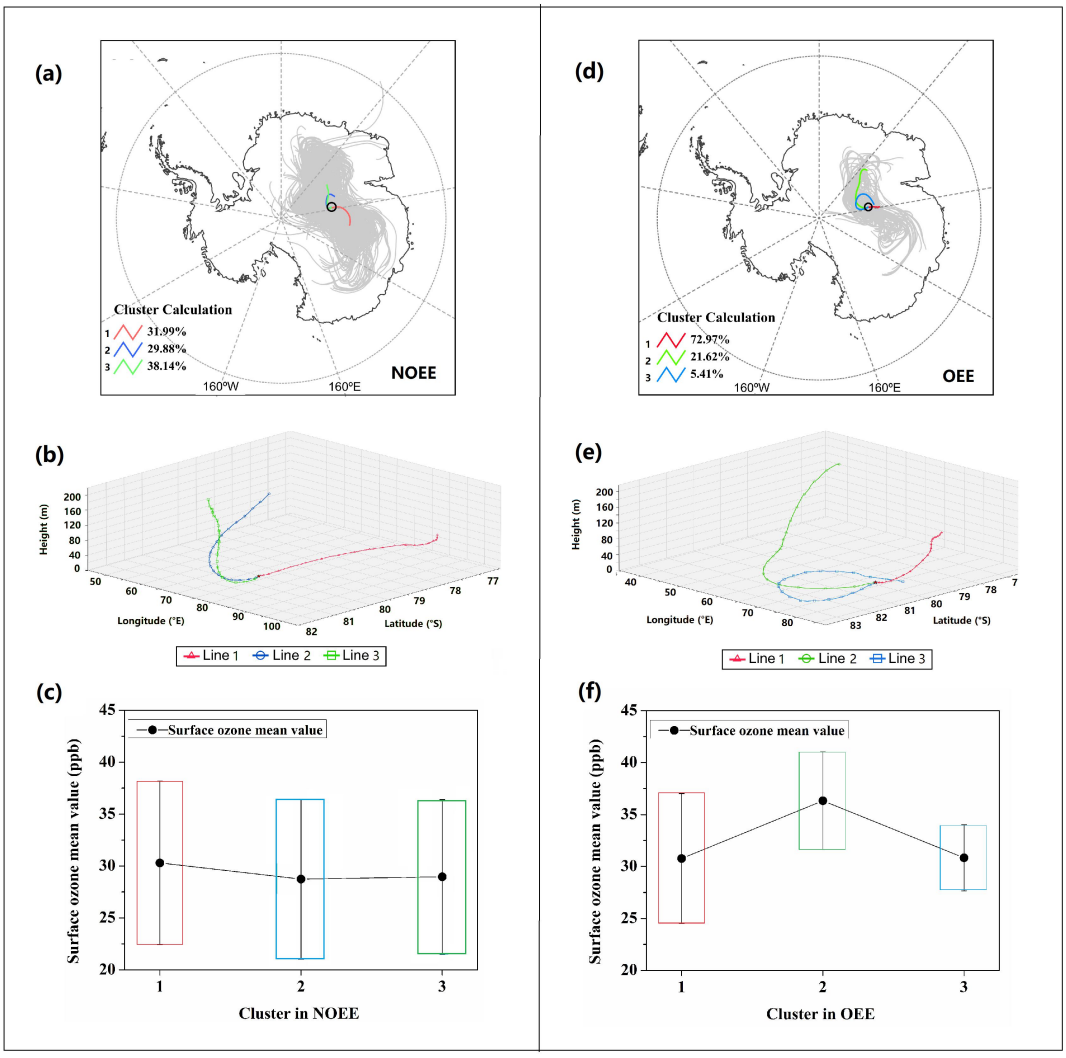

Figure 8: Backward HYSPLIT trajectories for each measurement day (gray lines in Figure 8a), and mean back trajectory for 3 HYSPLIT clusters (colored lines in Figure 8a, 3D view shown in Figure 8b) arriving at Kunlun Station during NOEEs. Subplot (c) shows the range of surface ozone concentrations measured at DA by cluster. Error bars are the standard deviation of the same cluster. Same as subplot (a, b, c), but subplot (d, e, f) for OEEs.

Year-round record of near-surface ozone and "O_3 Eenhancement Eevents" (OEEs) at Dome A, East Antarctica

Minghu Ding[1,2,*], Biao Tian[1,*], Michael C. B. Ashley[3], Davide Putero[4], Zhenxi Zhu[5], Lifan Wang[5], Shihai Yang[6], Chuanjin Li[2], Cunde Xiao[2, 7]

[1]State Key Laboratory of Severe Weather, Chinese Academy of Meteorological Sciences, Beijing 100081, China
[2]State Key Laboratory of Cryospheric Science, Northwest Institute of Eco-Environment and Resources, Chinese Academy of Sciences, Lanzhou 730000, China
[3]School of Physics, University of New South Wales, Sydney 2052, Australia
[4]CNR–ISAC, National Research Council of Italy, Institute of Atmospheric Sciences and Climate, via Gobetti 101, 40129, Bologna, Italy
[5]Purple Mountain Observatory, Chinese Academy of Sciences, Nanjing 210034, China
[6]Nanjing Institute of Astronomical Optics & Technology, Chinese Academy of Sciences, Nanjing 210042, China
[7]State Key Laboratory of Earth Surface Processes and Resource Ecology, Beijing Normal University, Beijing 100875, China
*These authors contributed equally to this work.
Correspondence to: Minghu Ding (dingminghu@foxmail.com)

Abstract. Dome A, the summit of the east Antarctic Ice Sheet, is an area challenging to access and is one of the harshest environments on Earth. Up until recently, long term automated observations from Dome A (DA) were only possible with very low power instruments such as a basic meteorological station. To evaluate the characteristics of near-surface O_3, continuous observations were carried out in 2016. Together with observations at the Amundsen-Scott Station (South Pole – SP) and Zhongshan Station (ZS, on the southeast coast of Prydz Bay), the seasonal and diurnal O_3 variabilities were investigated. The results showed different patterns between coastal and inland Antarctic areas that were characterized by high concentrations in cold seasons and at night. The annual mean values at the three stations (DA, SP and ZS) were 29.2 ± 7.5 ppb, 29.9 ± 5.0 ppb and 24.1 ± 5.8 ppb, respectively. We investigated the effect of specific atmospheric processes on near-surface summer O_3 variability, when O_3 enhancement events (OEEs) are systematically observed at DA (average monthly frequency peaking up to 64.5% in December). As deduced by a statistical selection methodology, these O_3 enhancement events (OEEs) are affected by a significant interannual variability, both in their average O_3 values and in their frequency. To explain part of this variability, we analyzed the OEEs as a function of specific atmospheric processes: (i) the role of synoptic-scale air mass transport over the Antarctic Plateau was explored using the Lagrangian back-trajectory analysis – Hybrid Single-Particle Lagrangian Integrated Trajectory (HYSPLIT) method and (ii) the occurrence of "deep" stratospheric intrusion events was investigated using the Lagrangian tool STEFLUX. The specific atmospheric processes, including synoptic-scale air mass transport, were analysed by the HYSPLIT back-trajectory analysis and the potential source contribution function (PSCF) model. Short-range transport accounted for the O_3 enhancement events (OEEs) during summer at DA, rather than efficient local production, which is consistent with previous studies of inland Antarctica. Moreover, the

identification of recent (i.e., 4-day old) stratospheric intrusions events by STEFLUX suggested that “deep” events only had a minor influence (up to 1.1 % of the period, in August) on “deep” events during the variability of near-surface summer O_3 at DA. The "deep" events during the polar night were significantly higher than those during the polar day. This work provides unique ~~information~~ data on ozone variation at DA and expands our knowledge of such events in Antarctica. Data are available at https://doi.org/10.5281/zenodo.3923517 (Ding et al., 2020).

Key words: near-surface O_3; Antarctica; OEE; STT;

1 Introduction

Ozone (O_3) is a natural atmospheric component that is found both in the stratosphere and troposphere and plays a major role in the atmospheric environment through radiative and chemical processes. O_3 does not have direct natural sources such as emission from the ground or vegetation, but rather is produced in the atmosphere, and its concentration ranges from a few ppb near the Earth’s surface to approximately a few ppm in the stratosphere. Stratospheric O_3, which is produced as a result of the photolysis of molecular oxygen, forms a protective layer against the UV radiation from the Sun. By contrast, throughout the troposphere and at the surface, O_3 is considered a secondary short-lived air pollutant (Monks et al., 2015), and O_3 itself is a greenhouse gas, such that a reduction in concentration has a direct influence on radiative forcing (Mickley et al., 1999; IPCC, 2013; Stevenson et al, 1998).

O_3 photochemical production in the troposphere occurs via hydroxyl radical oxidation of carbon monoxide (CO), methane (CH_4) and non-methane hydrocarbons (generally referred to as NMHC) in the presence of nitrogen oxides (NOx) (Monks et al., 2015). As these precursors are localized and their lifetimes are generally short, the distribution of near-surfaceO_3, which is produced from anthropogenic precursors, is also localized and time-variant. In the presence of strong solar radiation with $\lambda < 424$ nm, volatile organic compounds (VOCs) and NOx ($NO + NO_2$), O_3 is photochemically produced and can accumulate to a hazardous level during favourable meteorological conditions (Davidson, 1993; Wakamatsu et al., 1996). In the case of NOx-rich air, NO_2 is produced and accumulates via the reaction between NO and HO_2 or RO_2 (peroxy radicals), which is followed by the accumulation of O_3. However, in the case of NOx-poor air, these proxy radicals react with O_3 and lead to O_3 loss (Lin et al., 1988). Experiments conducted in Michigan (Honrath et al., 2000a) and Antarctica (Jones et al., 2000) found that NOx can be produced in surface snow. This production appears to be directly driven by incident radiation and photolysis of nitrate deposited in the snow (Honrath et al., 2000a, b).

Previous studies have shown that the near-surface O_3 of Antarctica may be influenced by a number of climate-related variables (Berman et al., 1999), such as the variation of UV flux caused by the variation of O_3 column concentration over Antarctica (Jones and Wolff, 2003; Frey et al., 2015), the accumulation and transport of long-distance, high concentration air masses (e.g., Legrand et al., 2016), and the depth of continental mixing layers. Many studies ~~has~~ have observed summer episodes of “O_3 enhancement events” (OEEs) in the Antarctic interior (e.g., Crawford et al., 2001; Legrand et al., 2009;

Cristofanelli et al., 2018), and they attributed this phenomenon to the NOx emissions from snowpack and subsequent photochemical O_3 production (for example, Jones et al., 2000). Moreover, this may provide an input source for the entire Antarctic region (for example, Legrand et al., 2016; Bauguitte et al., 2011). As the solar irradiance and the nitrate aerosol concentration increase, the emission of NO_X will increase through the photodenitrification process of the summer snowpack (e.g. $NO_3^- + hv \rightarrow NO_2 + O^-$; $O^- + H^+ \rightarrow OH$; Honrath et al., 2000; Warneck et al., 1989). ~~Indeed,~~ Helmig et al. (2008a,b) provided further insight into the vigorous photochemistry and O_3 production that result from the highly elevated levels of NOx in the Antarctic surface layer. During stable atmospheric conditions, which are typically observed during low wind and fair sky conditions, O_3 accumulated in the surface layer can reach up to twice its background concentration. Neff et al. (2008a) showed that shallow mixing layers associated with light winds and strong surface stability can be among the dominant factors leading to high NO levels. As shown by Cristofanelli et al. (2008) and Legrand et al. (2016), the photochemically-produced O_3 in the PBL over the Antarctic Plateau can affect the O_3 variability thousands of km away from the emission area, due to air mass transport.

The near-surface O_3 concentrations at high-elevation sites can also be increased by the downward transport of O_3-rich air from the stratosphere during deep convection and stratosphere-to-troposphere transport (STT) events. Moreover, the stratospheric O_3 in the polar regions can be transferred to the troposphere not only during intrusion events but also as a result of slow but prolonged subsidence (e.g., Gruzdev et al., 1993; Roscoe et al., 2004; Greenslade et al. 2017). The earliest studies, carried out by the aircraft flight NSFC-130 over the Ellsworth Mountains of Antarctica in 1978, found that mountainous terrain may induce atmospheric waves that propagate through the tropopause. The tropospheric and stratospheric air may be mixed, leading to an increase in the tropospheric O_3 concentration (e.g., Robinson et al., 1983). Radio soundings at the Resolute and Amundsen-Scott Stations also showed the existence of transport from the stratosphere to the troposphere, and the flux could reach up to 5×10^{10} mol/cm^2/s (e.g., Gruzdev et al., 1993). Recently, Traversi et al. (2014, 2017) suggested that the variability of air mass transport from the stratosphere to the Antarctic Plateau could affect the nitrate content in the lower troposphere and the snowpack.

Currently, the climatology of tropospheric O_3 over Antarctica is relatively understudied because observations of year-round near-surface O_3 have been tied to manned research stations. These stations are generally located in coastal Antarctica, except for the South Pole (SP) and Dome C continental stations on the East Antarctic Plateau. Thus, the only information currently available for the vast region between the coast and plateau are spot measurements of boundary layer O_3 during summer from scientific traverses (e.g., Frey et al., 2015) or airborne campaigns (e.g., Slusher et al., 2010). Moreover, the vertical profile of O_3 in the troposphere cannot be measured by satellites because the high density of O_3 in the stratosphere leads to the inaccurate estimation of tropospheric O_3 by limb-viewing sensors. Estimates of total O_3 in the troposphere have been made by subtracting the stratospheric O_3 column (determined by a limb-viewing sensor) from the total column of O_3 (measured by a nadir-viewing sensor) (Fishman et al., 1992). In other words, tropospheric profiles cannot be obtained by satellites, and we

cannot examine the spatial distribution of near-surface O_3 from space. As a result of these limitations, a dearth of information exists regarding the spatial gradient of near-surface O_3 across Antarctica and how it varies throughout the year.

To better understand the spatial variations and the source-sink mechanisms of near-surface O_3 in Antarctica, near-surface O_3 concentrations were measured during 2016 at Dome A (DA) and the Zhongshan Station (ZS). Together with records from the Amundsen-Scott Station (SP), we analysed specific processes that affect the intra-annual variability in surface O_3 over the East Antarctic Plateau; in particular, we determined (i) the synoptic-scale air mass transport within the Antarctic interior and (ii) the role of STT transport. This study broadens the understanding of the spatial and temporal variations in the near-surface O_3 concentration and transport processes that impact tropospheric O_3 over high plateaus.

2 Sites and methods description

2.1 Near-surface ozone observations

介绍测量 O3 的各种仪器，特别是三个站涉及到的仪器，及其优劣。DA, SP and ZS was used the Model 205 Dual Beam, Thremo 49C, and EC9810A and Model 205 ozone monitors, respectively. All three instruments are based on ultraviolet spectrophotometry to measure ozone concentration. The ultraviolet spectrophotometry is based on the law of Beer Lambert. The method of measuring ozone concentration by detecting the maximum absorption value of ozone at the wavelength of 253.7 nm. The principles are as follows:

$I = I_0 exp(-\alpha LC)$ (1)

The I I is the light intensity after the airflow passes through. The I_0 Io is the light intensity when the airflow does not pass through. The α a is the absorption coefficient. The L L is the absorption path, and the C C is the ozone concentration in the absorption gas.

Table 1 shows that there are great differences in measuring range, weight, working flow and data storage. Clearly, the Model 205 ozone monitor is smaller and portable, but the measuring range of the instrument is small and the data storage capacity is weak.These three monitors were made use of two detection cells to improve precision, baseline stability, and response time. In the dual beam instrument, UV light intensity measurements I (O_3-scrubbed air) and I_0 (unscrubbed air) are performed simultaneously. Combined with other improvements, The Model 205 Dual Beam Ozone Monitor is the fastest UV-based O_3 monitor on the market, with such small size, weight, and power requirements characteristics. Fast measurements are particularly desirable for unattended stations, aircraft and balloon measurements, where high spatial resolution is desired. The Model 205 Dual Beam Ozone Monitor (205 2B) is an Environmental Protection Agency (EPA) federal equivalent method (FEM).

There are ~~many~~several methods to measure the concentration of ozone, ~~such as~~including ultraviolet spectrophotometry, iodometry, sodium indigo disulfonate spectrophotometry, gas chromatography, chemiluminescence, fluorescence

spectrophotometry and long optical path differential absorption spectrometry, etc. (e.g. Wang et al.,2017). Of them the ultraviolet spectrophotometry is the most popular for~~At present, the main method used in~~ the surface ozone monitoring ~~is the ultraviolet spectrophotometry recognized and recommended by the international organization for standardization~~ and applied into ~~. There are~~ many commercial instruments ~~based on this method~~. The common ones such as Thermo 49C (Liu et al., 2006), API 400E (Sprovieri et al., 2003), ESA O342M (Lei et al., 2014), Ecotech 9810B (Moura et al., 2011), have been used in many regions for their larger measuring range and high precision, but they are expensive, need plenty of power supply and regular maintenance. Recently, more and more studies chosed the portable ozone monitors such as Model 205, Aeroqual Series 500, POM, due to its advantages of small volume, low price, low energy consumption and good applicability for field observation (e.g. Johnson et al., 2014; Lin et al., 2015; Sagona et al., 2018). In Antarctica, only few stations have carried out continuous ozone monitoring and all of them were equipped with the common types, that is Thermo/Ecotech types, as we know.

~~One is large-scale fixed monitoring instruments, mainly including Thermo 49C (Liu et al., 2006), API 400E (Sprovieri et al., 2003), ESA O342M (Lei et al., 2014), Ecotech 9810B (Moura et al., 2011), etc. This kind of instrument has large volume, high price, long measuring range, high precision, high energy consumption and needs regular maintenance. The other is portable monitor, mainly Model 205 (Johnson et al., 2014), Aeroqual Series 500 (Lin et al., 2015), POM (Sagona Jet al., 2018) etc. This kind of instrument has the advantages of small volume, low price, low energy consumption and good applicability for field observation.~~

~~At present, there are not many stations to carry out long-term near surface ozone observation in Antarctica. Because the operation of large fixed monitoring instruments requires continuous power supply and routine maintenance. Therefore, only a few countries' perennial stations (Syowa, Neumayer, Halley, Arrival Heights, South Pole, Zhongshan) have made continuous observations. The surface ozone data of some stations could be understood from the World Data Centre for Greenhouse Gases (WDCGG). However, there are few studies on the use of portable monitors for Antarctic ozone observation.~~

The Kunlun Station (80°25'02"S, 77°06'59"E, altitude 4087 m) is located in the DA area, on the summit of the east Antarctic Ice Sheet (~~Fig~~Figure~~ure~~ 1). The only continuous power supply is~~O_3 monitor is located at the PLATO Antarctic site testing observatory. The instrument was powered by~~ the PLATO-A observatory, ~~an improved version of the PLATO observatory described by Lawrence et al. (2009),~~ which can also provide~~d~~ internet access via the Iridium satellite network (detailed introduction of PLATO observatory can be found in Lawrence et al. (2009)). Due to the limitation of energy consumption and conditions encountered during transportation from coast to the Dome, larger monitors such as~~the~~ Thermo 49i ~~O_3 monitor~~ cannot be used. ~~A portable O_3 monitor with low energy consumption is suitable.~~Thus, ~~On~~ on the 1st of Jan 2016, we deployed a Model 205 Dual Beam Ozone Monitor (205 2B) during the 33rd Chinese National Antarctic Research Expedition. ~~The instrument is connected with outdoor filter through Teflon pipeline to prevent snow particles from blowing into the pipeline. The air inlet of the filter is located at the outdoor height of 4m. The instrument is set at the sampling frequency of~~

once an hour, and the data is transmitted to the observatory computer through RS232 and sent to Beijing by satellite.The instrumentModel 205 Dual Beam Ozone Monitor has been certified by Environmental Protection Agency and makes use of two detection cells to improve its precision, baseline stability, and response time. In the dual beam instrument, UV light intensity measurements I_0 (O_3-scrubbed air) and I (unscrubbed air) are performed simultaneously (Wang et al., 2017). AndCombined with other improvements, this instrumen it is the fastest UV-based O_3 monitor on the markettill now, with such a small size, light weight, and low power requirements characteristics (Ssupplementary Table S1). Especially, quick responseFast measurements are is particularly desirable for unattended stations, aircraft and balloon measurements, where high spatial resolution is desired. The Model 205 Dual Beam Ozone Monitor (205 2B) is an Environmental Protection Agency (EPA) federal equivalent method (FEM). In Dome A, we use Teflon pipeline to connect the free air at ~4m above surface with the instrument. At the inlet of the pipeline, a Thermo 47mm filter was used to prevent snow particles. During the observation, The instrument is connected with outdoor filter through Teflon pipeline to prevent snow particles from blowing into the pipeline. The air inlet of the filter is located at the outdoor height of 4m. Tthe instrument iswas set at the sampling frequency of once an hour, and the data iswas transmitted to the observatory computer through RS232 and sent to Beijing by satellite.每个站增加实验细节介绍。比如 DA，我们讲仪器安装在天文台的仪器仓里面，通过特氟龙管接到外面，离地面高度为 4-5m。中间有过滤葫芦头装置（虽然 DA 很洁净可能不需要）

The Zhongshan Station (69°22'12"S, 76°21'49"E, altitude 18.5 m) is located at the edge of the east Antarctic Ice Sheet (FigFigure ure 1),). TheAll instruments monitoring atmospheric chemistry observatory was constructedwere installed at the Swan Ridge observation room (69°22'12"S, 76°21'49"E, 18.5 m a.s.l.), northwest of the Nella fjord, at where we installed a UV absorption near-surface O3 analyzer (EC9810A) for long-term near-surface O_3 monitoring in Jan. 2008. The air inlet of the instrument was 4 m away fromabove the groundsurface, and connected to the indoor filterthe analyzer through the Teflon pipe, and connected to the monitor.where we installed a UV absorption near-surface O_3 analyzer (EC9810A) for long-term near-surface O_3 monitoring. The observational frequency was 3 min, and the data were transferred in real time to Beijing. Furthermore, to prevent data losses, a CR1000 data logger was used to record the data output in real time. Every three months, the O_3 analyzer was calibrated using the EC9811 O_3 calibrator, and 5 standard concentrations of O_3 gas were generated for each calibration. The calibration concentration and measured concentration underwent correlation analysis, and seasonal calibration results were generated every three months. In 2016, 5 calibrations were made, and the appropriate correlation coefficients (r) were all greater than 0.9995.

The Amundsen-Scott Station (89°59'51.19 "S, 139°16'22.41" E, altitude 2835 m) is located at the SP and operated by the United States. SP is one of the GAW station. In 2016, it was used thean Thermo 49C ozone monitor was used and 5-minute and 1-hour data was uploaded to GAW (Global Atmospheric Watch) every month. to upload the processed 5-minute and

~~1-hour frequency data every month.~~ The ~~near-surface O_3 data~~record used in this paper ~~were~~ was downloaded from the Earth System Research Laboratory Global Monitoring Division under the NOAA (https://www.esrl.noaa.gov/gmd/dv/data). The hourly data of these stations collated here are available at https://doi.org/10.5281/zenodo.3923517 (Ding et al., 2020).

2.2 Calibration process and results

Generally, the zero point, span point and operation parameters of the O_3 monitor should be checked before each operation. The zero point should be checked regularly during continuous observation. While such regular calibration was done at the Global Atmosphere Watch (GAW) and Zhongshan Station, it was not possible at DA due to the lack of logistic support and the extreme environment. To minimize the error and evaluate the accuracy of the experiment, a UV-absorption O_3 calibrator Thermo 49i-PS was used to examine the Model 205. The calibration procedure follows China's environmental protection standard "ambient air - Determination of ozone - ultraviolet method" (HJ590-2010) (http://www.mee.gov.cn/gkml/sthjbgw/sthjbgg/201808/t20180815_451411.htm) which is more strict than USEPA (Ref: USEPA . —Quality Assurance Handbook for Air Pollution Measurement Systems Volume II: Ambient Air Quality Monitoring Program[EB/OL].[2008-12-01]. http://www.epa.gov/ttn/amtic/files/ambient/pm25/qa/ QAHandbook-Vol-II.pdf.): the slope of calibration curve ranges between 0.95-1.05, and the intercept ranges between -5-5 ppb. Instruments used in the calibration process include a DOA-p512-bn air compressor (USA), in addition to the Thermo 49ips O_3 calibrator and the Model 205 O_3 monitor. Before each test, the O_3 calibrator and the O_3 monitor were turned on and preheated for 12 hours, and the measuring range was set to 400 ppb. We first generate a zero concentration using the Thermo 49ips and, once the analyzer response has stabilized on zero reading, we adjusted the Model 205's internal zero setting to matches the zero air source. Then, O_3 airflow at 400 ppb level was generated and injected into the analyzer, and a correction factor was calculated based on the observed value, which was then loaded into the Model 205 configuration.

After the calibration of the internal zero/span settings, a second stage of calibration was performed involving multi-point verification to check the response and stability of the analyzer. On Oct 5th 2015 (before the instrument was shipped) and May 6th 2017(the day that the instrument was transported back from Antarctica), a zero and 7 upscale points (0, 20, 35, 50, 65, 80, 100, 120 ppb) encompassing the full scale of the observation range (Table ~~S2~~12~~1~~), were generated by the Thermo 49ips to test the Model 205 analyzer. Each point was observed for 15 min, during the last 10 minutes of which readings were taken every minute of the calibrator and analyzer. Based on this experiment, the slope and intercept of the calibration curve were calculated by least squares. The results are shown in Table ~~2~~12, it can be concluded that the slopes of the linear correction curve were 0.99936 and 1.02520, and the intercepts were 0.53861 and 0.85220l ~~(Table 3~~222~~)~~, which fulfilled the requirements of HJ590-2010 and USEPA.

Another challenge when monitoring the atmosphere is the stability of the analyzer, which includes the analyzer's response time. Similarly with the regular calibration, it could not be performed during the observation period, but it was reassuring that the Model 205 was still in good condition when we did the multi-point verification in May 2017, as shown in Table

~~32~~32. The slope and intercept of the two calibration curves changed little and the standard uncertainties were small. To further test the stability, data consistency was also examined and the mean absolute deviation between two adjacent values was only 0.09 ppb. The largest difference was 0.61 ppb, indicating that the analyzer was stable and reliable.

Before analysis, a variance test was used to remove abnormal data based on the Laida criterion method, which assumes that the records obeyed a normal distribution. The formula is $xi - x > 3\sigma$, where xi is the measured value, x is the time series mean and σ is the standard deviation. After processing, 99.~~2~~3%, ~~91~~99.6%, and ~~99~~89.~~5~~3% of the hourly mean data were retained from the Amundsen-Scott Station, Zhongshan Station and Kunlun Station, respectively.

2.3 Air mass back-trajectory calculations

Gridded meteorological data for backward trajectories in Hybrid Single-Particle Lagrangian Integrated Trajectory (HYSPLIT) were obtained from the Global Data Assimilation System (GDAS-1) operated by the U.S. National Oceanic and Atmospheric Administration (NOAA) with 1°×1° horizontal resolution and 23 vertical levels, from 1000 hPa to 20 hPa (http://www.arl.noaa.gov/gdas1.php).

The HYSPLIT backward air mass trajectory model was previously applied to atmospheric research in Antarctica (Legrand et al., 2009; Hara et al., 2011). We used the HYSPLIT model in this paper to analyse the impact of varying air mass sources and the intrusion of stratospheric O_3. Backward trajectories and clusters were calculated using the US National Oceanic and Atmospheric Administration (NOAA)-HYSPLIT model (Draxler and Rolph, 2003; http://ready.arl.noaa.gov/HYSPLIT.php), which is a free software plug-in for MeteoInfo (Wang, 2014; http://meteothink.org/). The backward trajectories starting height was set at 20 m above the surface and the total run times was 120 hours for each backward trajectory, and each run was performed in time intervals of 6 hours (00:00, 06:00, 12:00, 18:00).

The integral error part of the trajectory calculation error can be estimated by simulating the backward trajectory at the end of the forward trajectory and comparing the differences of the tracks. The starting point of the backward integration is set as (77.12 ° E, 80.42 °S, 20m a.g.l.), the backward integration is 120 hours. Then the point reached at this time is taken as the starting point, and a forward simulation is made for 120h. In this simulation experiment, the contribution of integration error to trajectory calculation error is very small within the first 72 hours. With the extension of integration time, the integration error slightly increases.

The air mass trajectories were assigned to distinct clusters according to their moving speed and direction using a k-means clustering algorithm (Wong, 1979). Concerning with this study focused on transport pathway of O_3, the clustering result with the smallest number was selected as done by ~~(~~Wang et al.~~,~~ (2014). It was found ~~F~~three~~five~~ clusters performance best to represent~~ed~~ the meteorological characteristics of the transport pathways at DA. This number was then selected as the expected number of air mass trajectory clusters. A more detailed clustering procedure using the k-means algorithm can be found in Wang et al. (2014).

2.4 Potential source contribution function

The observation of a secondary maximum of O_3 in November–December at the inland Antarctic sites was first reported for the SP by Crawford et al. (2001), and was attributed to photochemical production induced by high NOx levels in the atmospheric surface layer, which were generated by the photo-denitrification of the Antarctic snowpack (same as Davis et al., 2001). At DC, a secondary maximum in November–December 2007 was also reported by Legrand et al. (2009), proving that photochemical production of O_3 in the summer takes place over a large part of the Antarctic Plateau. A further study by Legrand et al. (2016) found that the highest near-surface O_3 summer values were observed within air masses that spent extensive time over the highest part of the Antarctic Plateau before arriving at DC. To investigate the possible influence of synoptic-scale air mass circulation on the occurrence of OEEs at DA, 5-day HYSPLIT back-trajectories were analyzed (~~Figure~~Figure 9). We used the potential source contribution function (PSCF, see, e.g., Hopke et al., 1995; Brattich et al., 2017) to calculate the conditional probabilities and identify the geographical regions related to the occurrence of NOEEs and OEEs at DA (~~Figure~~Figure 7).

As in Yin et al. (2017), the potential source contribution function (PSCF) assumes that back trajectories arriving at times of high ~~mixing ratio~~concentrations likely point to significant pollution directions (Ashbaugh et al., 1985). This function was often applied to locate air masses associated with high levels of near-surface O_3 at different sites (Kaiser et al., 2007; Dimitriou and Kassomenos, 2015). In this study, the PSCF was calculated using HYSPLIT trajectories. The top of the model was set to 10000 m a.s.l. The PSCF values for the grid cells in the study domain were calculated by counting the trajectory segment endpoints that terminated within each cell (Ashbaugh et al., 1985). If the total number of end points that fall in a cell is n_{ij} and there are m_{ij} points for which the measured O_3 parameter exceeds a criterion value selected for this parameter, then the conditional probability, the PSCF, can be determined as

$$\mathrm{PSCF}_{ij} = \frac{m_{ij}}{n_{ij}} \qquad (1)$$

The concentrations of a given analyte greater than the criterion level are related to the passage of air parcels through the ijth cell during transport to the receptor site. That is, cells with high PSCF values are associated with the arrival of air parcels at the receptor site, which has near-surface O_3 concentrations that are higher than the criterion value. These cells are indicative of areas with 'high potential' contributions of the constituent. Identical PSCF_{ij} values can be obtained from cells with very different counts of back-trajectory points (e.g., grid cell A with $m_{ij} = 5000$ and $n_{ij} = 10000$ and grid cell B with $m_{ij} = 5$ and $n_{ij} = 10$). In this extreme situation, grid cell A has 1000 times more air parcels passing through it than grid cell B. Because the particle count in grid cell B is sparse, the PSCF values in this cell are highly uncertain. To explain expound the uncertainty due to the low values of n_{ij}, the PSCF values were scaled by a weighting function W_{ij} (Polissar et al., 1999).

The weighting function reduced the PSCF values when the total number of endpoints in a cell was less than approximately 3 times the average number of end points per cell. In this case, Wij was set as follows:

$$W_{ij(NOEE)} = \begin{cases} 1.00 & nij > 12Nave \\ 0.70 & 12Nave > nij > 3Nave \\ 0.42 & 3Nave > nij > 1.5Nave \\ 0.05 & Nave > nij \end{cases} \quad (2)$$

$$W_{ij(OEE)} = \begin{cases} 1.00 & nij > 8Nave \\ 0.70 & 8Nave > nij > 2Nave \\ 0.42 & 2Nave > nij > 1Nave \\ 0.05 & Nave > nij \end{cases} \quad (3)$$

where Nave represents the mean nij of all grid cells. The weighted PSCF values were obtained by multiplying the original PSCF values by the weighting factor.

3 Near-surface O_3 variability

3.1 Mean concentration

At the DA, SP, and ZS sites, the annual mean ~~molar ratio~~concentrations of near-surface O_3 were 29.2 ± 7.5 ppb, 29.9 ± 5.0 ppb and 24.1 ± 5.8 ppb, respectively; the maximum annual mean ~~molar ratio~~concentration reached 42.5 ppb, 46.4 ppb and 32.8 ppb, respectively; and the minimum annual mean ~~molar ratio~~concentrations were 14.0 ppb, 10.9 ppb and 9.9 ppb, respectively. The inland stations are characterized by higher annual mean ~~molar ratio~~concentrations than the coastal station. There were also obvious differences between polar day and polar night at all stations. In ~~Figure~~Figure 2, we define the polar day and night windows by the day of year margins and have used different shading colours to identify the polar day and polar night. The average ~~molar ratio~~concentrations of near-surface O_3 during polar night at the DA, SP and ZS sites were 34.1 ± 4.3 ppb, 31.5 ± 3.9 ppb and 28.7 ± 1.3 ppb, respectively, and much lower concentrations appeared during non-polar night, with corresponding values of 26.1 ± 7.0 ppb, 28.1 ± 5.8 ppb and 23.1 ± 5.9 ppb, respectively. Interestingly, the SP had the highest near-surface O_3 concentration during non-polar night, whereas at DA the highest concentration occurred during polar night and the largest variation occurred at this site.

3.2 Seasonal variation

In this part, we define Oct-Mar as the warm season and Apr-Sep~~t~~ as the cold season, which is similar to the definition of polar day and night.

In agreement with previous studies (Oltmans et al., 1976; Gruzdev et al., 1993; Ghude et al., 2005), the concentrations of near-surface O_3 at the three stations were high and less variable during the cold season and low and more variable during the warm season (Figure 3). In Antarctica, the emissions of O_3 precursors are generally less than those at mid and low latitudes, whereas ultraviolet radiation is relatively strong; thus, when solar radiation occurs, the depletion effect is much greater than the effects from photochemical reactions during the warm season (Schnell et al., 1991). As explained by previous studies, during the polar night, due to the lack of light, the photochemical reactions stop. Moreover, due to the lack of loss effect, the O_3 concentration gradually increased and the fluctuations became smaller. During the polar night, the monthly variation of surface O_3 at ZS was lower than that at the DA but higher than that at the SP. However, due to strong UV radiation in the low latitude areas and the presence of bromine-controlled O_3 depletion events in coastal areas, the ZS shows a large seasonal variations during the non-polar night (Wang et al., 2011; Prados-Roman et al., 2017). However, at the SP Station, the largest standard deviation was observed in December, similarly to the characteristics at Dome-C station (DC) from November to December (Legrand et al., 2009; Cristofanelli et al., 2018). Figures 2 and 3 indicate that the near-surface O_3 showed obviously larger variations at the DA than the SP during the polar night, since, due to the different geographical location, the meteorological conditions of DA and SP are different. The abnormal fluctuation of O_3 concentration over the DA during the polar night may be related to its special geographical environment.

As mentioned in the introduction section, mountainous topography/mountain waves may disturb advection transport in the stratosphere and lead to downward transportation to the troposphere (Robinson et al., 1983). DA is on the summit of the east Antarctic Ice Sheet, and the tropospheric depth is only ~4.6 km (Liang et al., 2015), which favours exchange between the stratosphere and troposphere. However, the topography in this area is very flat and creates a disadvantage for mountain waves. Does O_3 transport occur? We will analyse and discuss this question in section 4.

3.3 Diurnal variation

To characterize the typical monthly O_3 diurnal variations at the three stations, we analysed the mean diurnal variations of O_3 at the three stations (Figure 4) and the standard deviation of the mean diurnal variations (Figure 5). At the DA site, the mean diurnal concentrations for each month were relatively steady, with the standard deviation of the mean diurnal concentration for each month being lower than 0.4 ppb. At the SP, the mean diurnal concentrations were less variable as well. Except for December, the standard deviation of the mean diurnal concentration was lower than 0.3 ppb. At ZS, except for October, the standard deviation of the mean diurnal concentration was greater than that at the other two stations. In particular, the standard deviation of the mean diurnal concentration of ZS in September, November and December exceeded 0.5 ppb. ~~This difference may be related to the different distance to coastal line. As a coastal station, Zhongshan station often have ozone depletion episodes (ODEs) in spring. Along with the change of meteorological conditions, including the decrease of temperature, the change of wind direction from east to north, and the decrease of wind speed. As a result, a large amount of O_3 is consumed by the high concentration BrO air mass over the sea ice area, resulting in the occurrence of ODE in the~~

station area. However, due to the influence of polar vortices, ODEs of inland stations are not obvious (Wang Y et al., 2011; Ye et al., 2018)..Obviously, the average daily concentration fluctuation in Zhongshan station was obviously different with the two inland stations, which can be attributed into their background climates. In Spring, ODEs occur frequently at Zhongshan Station. And this phenomenon always accompanies with abrupt weather transit from continental dominant to oceanic dominant, in other words, the BrO brought by northerly wind from sea ice area could leaded to serious ozone depletion (Wang Y et al., 2011; Ye et al., 2018). Whereas at inland stations like DA and SP, there were rarely ODEs.

On the whole, tThe mean diurnal variations in different time periods were not obvious, and the mean diurnal concentrations of the three stations fluctuated within a range of less than 1 ppb, indicating that daily photochemistry reactions were not the dominant factor in near-surface O_3 at the three stations. The magnitude of the diurnal variation was low, which is similar to the variations found atof other Antarctic stations,,Neumayer Dome C and Marambio McMurdo for instance (Gruzdev et al., 1993; Ghude et al., 2005; NadzirOltmans et al., 2010 8).

4 Ozone under OEEs at the Kunlun Station

4.1 Identification of OEEs

Our method to select the days characterized by OEEs is based on the procedure used in Cristofanelli et al. (2018). First, a sinusoidal fit is used to calculate the O_3 annual cycle not affected by the OEEs, then a probability density function (PDF) of the deviations from the sinusoidal fit is calculated, with the application of a Gaussian fit to the obtained PDF. As reported in Giostra et al. (2011), the deviations from the Gaussian distribution (calculated by using the Origin 9© statistical tool) can be used to identify observations affected by non-background variability. We computed the further Gaussian fitting of PDF points beyond 1 σ (standard deviation) of the Gaussian PDF, and determined the non-background O_3 daily values that may be affected by "anomalous" O_3 enhancement. The intersection of the two fitting curves is taken as our screening threshold (3.4 ppb at SP, 3.4 ppb at Da and 2.5 ppbzs at ZS). Figures 6a, 6b and 6c show OEE days and NOEE days at these three stations, while Figures 6d, 6e and 6f report the distribution frequency of OEE days.

In total, 42 days at DA were found to be affected by anomalous OEEs: 14.3% in January, 2.4% in May, 14.3% in June, 4.8% in July, 11.9% in August, 4.8% in November and 47.6% in December (Figure 6e, blue bars). This result clearly indicates that half of the anomalous days occurred in December, followed by January and June. At SP, 36 days with OEEs were found in 2016: 44.4% in January, 30.6% in November, and 25% in December (Figure 6d, grey bars). Apparently, OEEs occur only in summertime at this measurement site. ZS was characterized by more days with OEEs: 53 days in April (34.0%), followed by September (18.9%), January (13.2%), October (11.3%), November (11.3%), December (5.7%) March (3.8%) and May (1.9%) (Figure 6f, yellow bars).from the results above, "it can be seen that" SP was characterized....

From the results above, it can be seen that SP was characterized by concentrated OEE occurrences, and ZS had the most scattered OEEs pattern. In addition, all OEEs at SP and ZS occurred during the Antarctic warm season, and no OEEs were present during the polar night, similarly to the pattern observed at DC (Cristofanelli et al., 2018). In contrast, the OEEs also occurred during the polar night in DA, and the number of OEE occurrence days accounted for up to 33% of the total number of events throughout the year. This is the main reason ~~in the section 3.2 for~~of the large variations of daily average concentration~~, in which~~ during the polar night of DA ~~in the section 3.2~~.

Previous studies (e.g., Legrand et al., 2016; Cristofanelli et al., 2018) carried out in DC showed that the O_3 variability at DC could be associated with processes occurring at long temporal scales. In addition, the accumulation of photochemically produced O_3 during transport of air masses was the main reason for OEEs, whereas the stratospheric intrusion events had only a minor influence on OEEs (up to 3%). This finding cannot explain the temporal occurrence pattern of OEEs at DA. To determine the unknown cause, we investigated the synoptic-scale air mass transport and the STT occurrence at the measurement site.

4.2 Role of synoptic-scale air mass transport

During NOEEs, the air masses arriving at DA mainly come from the west and east of DA, and the 3-D clusters show that the air masses travelled over the Antarctic plateau before reaching DA (~~Fig.~~Figure 8b). The difference in the number of the three cluster trajectories is small, and the difference in the corresponding cluster average concentrations is not large. Using the PSCF results, we have identified air masses associated with higher surface ozone at DA during NOEEs (~~Fig.~~Figure 8a). The Antarctic Plateau to the east and west of DA had high PSCF weight values (Figure 7), which shows that, during NOEEs, the potential source area of surface O_3 for DA is mainly in the inland plateaus in the east and west, and the area of high PSCF weight values distribution in the east is more larger than other directions.

Compared with NOEEs, the clustering results of trajectories during OEEs have different characteristics. In OEEs, the air masses that arrived at DA were ~~predominantly~~prevalent from the north and from the west, and the 3-D clusters indicated that the 73% of the air mass trajectories came from the area north of DA (red line in ~~Fig.~~Figure ~~9a~~8e). The average concentrations of the three clusters differ greatly (~~Fig.~~Figure ~~8~~9~~f~~e), but they are all higher than those obtained for NOEEs. It should be noted that 68% of Line-2 cluster (green line in ~~Fig.~~Figure ~~8~~9~~d~~a) occurred during the polar night (~~Fig.~~Figure ~~10~~9) and had a high average O_3 concentration (reached 36.3 ppb). This shows that the OEEs of the polar night are more affected by the high value O_3 air masses over the plateau west of DA than those during the polar day. Using the PSCF results, during OEEs, we did not find a large area of high WPSCF value, the high WPSCF value only appeared in the east and the north of DA over a limited area. However, independently on the polar day or on the polar night, the Line-1 cluster trajectory accounted for more than 60% during OEEs. In addition, the short distance of Line-1 cluster trajectory indicates that the air mass transport speed is slow, which is conducive to the accumulation of O_3 along the way. It can be seen from Figure ~~9b~~ ~~8b~~c~~e~~ that the characteristic values of backward trajectory clustering during OEEs are mostly lower than 200 m a.g.l. (supporting

the role of snow as the source of near surface O_3). As Fiebig et al. (2014) ha~~ves~~ proposed, the increase of O_3 values in the near surface of central Antarctica may also be related to the transport of free tropospheric air and aged pollution plumes from low latitudes. In addition, Figure ~~11~~ 10 shows that the average O_3 growth rate reached 0.29 ppb/h during OEEs in polar night, while the average O_3 growth rate was -0.06 ppb/h during NOEEs in polar night (Figure ~~11~~10). The statistical scatter distribution showed that 97% of OEEs occurred when the wind speed was lower than 4 m/s. The overall average wind speed during OEEs is also significantly lower than that of NOEEs. As Helmig et al. (2008a) have proposed, during stable atmospheric conditions (which typically existed during low wind and fair sky conditions) ozone accumulates in the surface layer and its concentration increases rapidly.

This finding confirms that the OEEs of DA are mainly caused by the accumulation of high concentrations of air masses transported occurring nearby, and the synoptic-scale transport can favor the photochemical production and the accumulation of O_3 accumulation by air masses travelling over the plateau near the north of DA before their arrival.

4.3 Role of STT events

4.3.1 Identification of "deep" STT events

Several methods can be applied to study stratosphere-to-troposphere transport (STT) events. One method is the chemistry-climate hindcast model GFDL-AM3, which Lin et al. (2017) used to evaluate the increasing anthropogenic emissions in Asia, and Xu et al. (2018) used to examine the impact of direct tropospheric ozone transport at the Waliguan Station. Stratosphere-to-Troposphere Exchange Flux (STEFLUX, Putero et al., 2016) is a novel tool to quickly obtain reliable identification of STT events occurring at a specific location and during a specified time window. STEFLUX relies on a compiled stratosphere-to-troposphere exchange climatology, making use of the ERA-Interim reanalysis dataset from the ECMWF, and a refined version of a well-established Lagrangian methodology. STEFLUX is able to detect stratospheric intrusion events on a regional scale, and it has the advantage of retaining additional information concerning the pathway of stratosphere-affected air masses, such as the location of tropopause crossing and other meteorological parameters along the trajectories.

We applied STEFLUX to assess the possible contribution of STT to near-surface O_3 variability in the DA region (i.e., STEFLUX "target box", for further details on the methodology see Putero et al., 2016), and for identifying the measurement periods possibly affected by "deep" STT events (i.e., stratospheric air masses transferred down to the lower troposphere). For this work, we set the top lid of the box at 500 hPa, and the following geographical boundaries: 79–82 °S, and 76–79 °E. A "deep" STT event at Kunlun Station was determined if at least 1 stratospheric trajectory crossed the 3-D target box ~~(eg. Table S2 is the result of "deep" STT screened by STEFLUX tool.)~~.

4.3.2 Role of STT events at DA

The possible occurrence of stratospheric intrusion events, and their role in affecting the variability of near-surface O_3 and tropospheric air-chemistry in Antarctica has been investigated in several studies (Murayama et al., 1992; Roscoe, 2004; Stohl and Sodemann, 2010; Mihalikova and Kirkwood, 2013; Traversi et al., 2014; Traversi et al., 2017; Cristofanelli et al., 2018). To provide a systematic assessment of the possible influence of "deep" STT events to the near-surface O_3 variability at Kunlun Station, we used the STEFLUX tool (see Sect. 4.3.1). Figure ~~12~~ 11 shows the distribution of the occurrence of "deep" STT events over DA during the year. Although it is difficult to see a clear seasonal cycle, due to the low frequency of "deep" STT events, our results are in agreement with previous studies, indicating STT influence of up to 2% on a monthly basis (Stohl and Sodemann, 2010; Cristofanelli et al., 2018). According to our STEFLUX outputs, the highest frequency of "deep" STT events was observed in May and August (1.1%). The frequency of occurrence of "deep" STT events identified by STEFLUX at Kunlun Station is about one order of magnitude lower than the occurrence of OEEs. Thus, a direct link of STT with OEEs interannual variability is unlikely, as also reported for DC station (Cristofanelli et al., 2018). Nevertheless, STT events can be a source of nitrates for the Antarctic atmosphere through different processes, thus indirectly affecting near-surface O_3 concentrations and favouring the presence of OEEs (Traversi et al., 2014; 2017).

5 Summary

Based on the in-situ monitoring data during 2016 at DA, the variation, formation, and decay mechanisms of near-surface O_3 were studied and compared with those at SP and ZS stations. The annual mean concentrations of near-surface O_3 at the DA, SP and ZS sites were 29.2 ± 7.5 ppb, 29.9 ± 5.0 ppb, and 24.1 ± 5.8 ppb, respectively. The near-surface O_3 concentrations were clearly higher in winter/polar night, with small fluctuations, than in the other seasons, which is different from the patterns observed at low latitudes. The O_3 in inland areas was also higher than over the coast.

The diurnal variations showed nonsignificant regular patterns, and the range of the average diurnal concentration fluctuation was less than 1 ppb at all three stations. These findings suggest that the synoptic transport somehow controls the overall O_3 variability, as has been shown at the SP~~Amundsen-Scott~~ and DC stations (Neff et al., 2008b; Cristofanelli et al., 2018).

At Kunlun station, it is unlikely that there is a direct relationship between STT and OEEs. The frequency of deep STT events identified by STEFLUX is about an order of magnitude lower than OEEs, and reaches its highest frequency (1.1%) in May and August. As deduced by the STEFLUX application, "deep" STT events play a marginal role in steering the occurrence of OEEs at DA via "direct" transport of O_3 from the stratosphere/the free troposphere, to the surface. As explained in Cristofanelli et al. (2018), this can be related to an underestimation of STT "young" (i.e., < 4-day old) events by STEFLUX, or to insufficient spatial and vertical resolution from ERA-Interim to fully resolve the complex STT transport in the Antarctic atmosphere (Mihalikova and Kirkwood, 2013). Despite this, STT can still represent a source of nitrates for the

Antarctic snowpack, thus possibly affecting summer photochemical O_3 production. Therefore, it is important to carry out further studies to better assess these processes.

The characteristics and mechanisms of near-surface O_3 revealed in this paper have important implications for better understanding the formation and decay processes of near-surface O_3 in Antarctica, especially over the plateau areas. Nevertheless, the lack of observations restricted our ability to amass more information. Long-term sustained observations at Dome A, Dome C, Dome F, SP, Vostok, and other locations, would greatly help in the future. ~~In addition, the atmospheric chemical models are also valuable (Lin et al., 2017; Xu et al., 2018). In the future, we will compare and analyze different atmospheric chemical models and methods to obtain a more accurate analysis of the OEEs in Antarctica.~~

6 Data availability

All data presented in this paper are available in https://doi.org/10.5281/zenodo.3923517 (Ding et al., 2020). The data set covers the hourly average concentrations of near-surface ozone at three stations (i.e. SP, ZS, DA).

Author contribution

Minghu Ding and Biao Tian designed the experiments and wrote the manuscript; Minghu Ding carried out the experiments; Biao Tian analyzed the experimental results. Minghu Ding, Biao Tian and Davide Putero revised the manuscript; Davide Putero run the STEFLUX tool. Michael Ashley, Zhenxi Zhu, Lifan Wang, Shihai Yang, Jie Tang, Chuanjin Li, Cunde Xiao and discussed the results.

Acknowledgements:

This work is financially supported by the National Natural Science Foundation of China (41771064), the Strategic Priority Research Program of Chinese Academy of Sciences (XDA20100300) and the Basic Fund of the Chinese Academy of Meteorological Sciences (2018Z001). The observations were carried out by during the Chinese National Antarctic Research Expedition at the Zhongshan Station and the Kunlun Station. We are also grateful to NOAA for providing the HYSPLIT model and GFS meteorological files. Yaqiang Wang is the developer of MeteoInfo and provided generous help for the paper. PLATO-A was supported by the Australian Antarctic Division and with NCRIS funding through Astronomy Australia Limited.

References

Ashbaugh, L. L., Malm, W. C., and Sadeh, W. Z.: A residence time probability analysis of sulfur concentrations at Grand Canyon National Park, Atmos. Environ., 19, 1263–1270, https://doi.org/10.1016/0004-6981(85)90256-2, 1985.

Bauguitte, S. J. B. , Jones, A. E. , Hutterli, M. A. , Anderson, P. S. , Maxfield, D. J. , Roscoe, H. K. , Wolff, E. W. , Virkkula, A. , Kirkwood, S. and Weller, R. : Preliminary data analysis from the IPY autonomous surface ozone monitoring network in Dronning Maud Land, Antarctica , EGU General Assembly , 2009.

Berman S., Ku J Y., Rao S T.: Spatial and Temporal Variation in the Mixing Depth over the Northeastern United States during the Summer of 1995, Journal of Applied Meteorology, 38(12):1661-1673, https://doi.org/10.1175/1520-0450(1999)038<1661:SATVIT>2.0.CO;2, 1999.

Brattich, E., Orza, J.A.G., Cristofanelli, P., Bonasoni, P., Tositti, L.: Influence of stratospheric air masses on radiotracers and ozone over the central Mediterranean, J. Geophys. Res.: Atmosphere, https://doi.org/10.1002/2017JD027036, 2017.

Crawford, J. H., Davis, D. D., Chen, G., Buhr, M., Oltmans, S., Weller, R., Mauldin, L., Eisele, F., Shetter, R., Lefer, B., Arimoto, R., Hogan, A.: Evidence for photochemical production of ozone at the South Pole surface, Geophysical Research Letters, 28(19), 3641-3644, https://doi.org/10.1029/2001gl013055, 2001.

Cristofanelli, P., Bonasoni, P., Calzolari, F., Bonafè, U., Lanconelli, C., Lupi, A., Trivellone, G., Vitale, V., Petkov, B.: Analysis of near-surface ozone variations in terra nova bay, Antarctica, Antarctic Science, 20(04), 415-421, http://dx.doi.org/10.1017/S0954102008001028, 2008.

Cristofanelli, P., Calzolari, F., U. BONAFè, Lanconelli, C., Lupi, A., & Busetto, M.: Five-year analysis of background carbon dioxide and ozone variations during summer seasons at the mario zucchelli station (antarctica), Tellus. Series B: Chemical and Physical Meteorology, 63(5), 831-842, https://doi.org/10.1111/j.1600-0889.2011.00576.x, 2011.

Cristofanelli, P., Putero, D., Bonasoni, P., Busetto, M., Calzolari, F., Camporeale, G., Paolo , C., Giuseppe, L., Angelo, P., Boyan, T., Rita, U., Roberto, V.: Analysis of multi-year near-surface ozone observations at the wmo/gaw “concordia” station (75°06 ′ s, 123°20 ′ e, 3280m a.s.l. – antarctica), Atmospheric Environment, 177, 54-63, https://doi.org/10.1016/j.atmosenv.2018.01.007, 2018.

Davis, D. D., Nowak, L. B., Chen, G., Buhr, M., Arimoto, R., Hogan, A., Eisele, F., Mauldin, L., Tanner, D., Shetter, R., Lefer, B., and McMurry, P.: Unexpected high levels of NO observed at South Pole, Geophys. Res. Lett., 28, 3625–3628, 2001.

Davidson A.: Update on ozone trend in California's south coast air basin, Journal of the Air & Waste Management Association, 43, 226–227, https://doi.org/10.1080/1073161x.1993.10467130, 1993.

Dimitriou, K., Kassomenos, P.: Three year study of tropospheric ozone with back trajectories at a metropolitan and a medium scale urban area in Greece, Sci. Total Environ., 502, 493–501, https://doi.org/10.1016/j.scitotenv.2014.09.072, 2015.

Ding, M., Tian, B.: The surface ozone observation data of Kunlun station in 2016 [Data set], Zenodo, http://doi.org/10.5281/zenodo.3923517, 2020.

Draxler, R. R., Rolph, G. D.: HYSPLIT (HYbrid Single-Particle Lagrangian Integrated Trajectory) Model, NOAA Air Resour, Lab., Silver Spring, Md. (Available at http://www.arl.noaa.gov/ready/hysplit4.html), 2003.

Fiebig, M., Hirdman, D., Lunder, C. R., Ogren, J. A., Solberg, S., Stohl, A., and Thompson, R. L.: Annual cycle of Antarctic baseline aerosol: controlled by photooxidation-limited aerosol formation, Atmos. Chem. Phys., 14, 3083–3093, https://doi.org/10.5194/acp-14-3083-2014, 2014.

Frey, M. M., Roscoe, H. K., Kukui, A., Savarino, J., France, J. L.,King, M. D., Legrand, M., Preunkert, S.: Atmospheric nitrogen oxides (NO and NO2) at Dome C, East Antarctica, during the OPALE campaign, Atmos. Chem. Phys. 15(14), 7859-7875. https://doi.org/10.5194/acp-15-7859-2015, 2015.

Fishman J , Brackftt V G , Fakhruzzaman K .: Distribution of tropospheric ozone in the tropics from satellite and ozonesonde measurements, Journal of Atmospheric & Terrestrial Physics, 54(5):589-597, 1992.

Giostra, U., Furlani, F., Arduini, J., Cava, D., Manning, A., ODoherty, S., Reimann, S., Maione, M.: The determination of a "regional" atmospheric background mixing ratio for anthropogenic greenhouse gases: a comparison of two independent methods, Atmos. Environ. 45, 7396–7405, https://doi.org/10.1016/j.atmosenv.2011.06.076, 2011.

Greenslade, J. W., Alexander, S. P., Schofield, R., Fisher, J. A., and Klekociuk, A. K.: Stratospheric ozone intrusion events and their impacts on tropospheric ozone in the Southern Hemisphere, Atmos. Chem. Phys., 17, 10269–10290, https://doi.org/10.5194/acp-17-10269-2017, 2017.

Gruzdev, A. N., Sitnov, S. A.: Tropospheric ozone annual variation and possible troposphere-stratosphere coupling in the arctic and antarctic as derived from ozone soundings at resolute and amundsen-scott stations, Tellus. Series B: Chemical and Physical Meteorology, 45(2), 89-98, https://doi.org/10.1034/j.1600-0889.1993.t01-1-00001.x, 1993.

Ghude, S. D., Kumar, A., Jain, S. L., Arya, B. C., Bajaj, M. M.: Comparative study of the total ozone column over maitri, antarctica during 1997, 2002 and 2003, International Journal of Remote Sensing, 26(16), 3413-3421, https://doi.org/10.1080/01431160500076434, 2005.

Hara, K., Osada, K., Nishita-Hara, C., and Yamanouchi, T.: Seasonal variations and vertical features of aerosol particles in the Antarctic troposphere, Atmospheric Chemistry and Physics, 11(11), 5471-5484, https://doi.org/10.5194/acp-11-5471-2011, 2011.

Helmig, D. , Johnson, B. , Samuel, J. , Oltmans, Neff, W. , Eisele, F.: Elevated ozone in the boundary layer at south pole, Atmospheric environment, 42(12), p.2788-2803, https://doi.org/10.1016/j.atmosenv.2006.12.032, 2008a.

Helmig, D. , Johnson, B. J. , Warshawsky, M. , Morse, T. , Neff, W. D. , Eisele, F.: Nitric oxide in the boundary-layer at south pole during the antarctic tropospheric chemistry investigation (antci), Atmospheric Environment, 42(12), https://doi.org/2817-2830,10.1016/j.atmosenv.2007.03.061, 2008b.

Honrath, R. E., Guo, S., Peterson, M. C., Dziobak, M. P., Dibb, J. E., and Arsenault, M. A.: Photochemical production of gas phase NO x from ice crystal NO3−, Journal of Geophysical Research: Atmospheres, 105(D19), 24183-24190, https://doi.org/10.1016/j.10.1029/2000JD900361,2000a.

Honrath, R. E., Peterson, M. C., Dziobak, M. P., Dibb, J. E., Arsenault, M. A., and Green, S. A.: Release of NOx from sunlight - irradiated midlatitude snow, Geophysical Research Letters, 27(15), 2237-2240, https://doi.org/10.1029/1999GL011286, 2000b.

Hopke, P.K., Barrie, L.A., Li, S.-M., Cheng, M.-D., Li, C., Xie, Y.: Possible sources and preferred pathways for biogenic and non-sea-salt sulfur for the high Arctic. J. Geophys. Res.: Atmosphere 100, 16595–16603, https://doi.org/10.1029/95JD01712, 1995.

IPCC. Summary for policymakers[M] // Climate Change 2013: The Phsical Science Basis. Contribution of Working Group to the fifth assessment report of the Intergov-ernmentai Panelon Climate Change. Cambridge & New York: Cambridge University Press, 2013.

Jones, A. E., Weller, R., Wolff, E. W., and Jacobi, H. W.: Speciation and rate of photochemical NO and NO2 production in Antarctic snow, Geophysical Research Letters, 27(3), 345-348, https://doi.org/10.1029/1999GL010885, 2000.

Jones, A.E., Wolff, E.W.: An analysis of the oxidation potential of the South Pole boundary layer and the influence of stratospheric ozone depletion, Journal of Geophysical Research, 108(D18):4565, https://doi.org/10.1029/2003JD003379, 2003.

Johnson T., Capel J., Ollison W.: Measurement of microenvironmental ozone concentrations in Durham, North Carolina, using a 2B Technologies 205 Federal Equivalent Method monitor and an interference-free 2B Technologies 211 monitor, Journal of the Air & Waste Management Association, 64(3):360-371, https://doi.org/10.1080/10962247.2013.839968, 2014.

Kaiser, A., Scheifinger, H., Spangl, W., Weiss, A., Gilge, S., Fricke, W., Ries, L., Cemas, D., and Jesenovec, B.: Transport of nitrogen oxides, carbon monoxide and ozone to the alpine global atmosphere watch stations Jungfraujoch (Switzerland), Zugspitze and Hohenpeißenberg (Germany), Sonnblick (Austria) and Mt.Krvavec (Slovenia), Atmos. Environ., 41, 9273–9287, https://doi.org/10.1016/j.atmosenv.2007.09.027, 2007.

Lawrence, J. S., Ashley, M. C. B., Hengst, S., Luong-Van, D. M., Storey, J. W. V., Yang, H., Zhou, X., and Zhu, Z.: *The PLATO Dome A site testing observatory: power generation and control systems*, Review of Scientific Instruments, 80, 064501-1–064501-10, 2009.

Legrand, M., Preunkert, S., Jourdain, B., Gallée, H., Goutail, F., Weller, R., and Savarino, J.: Year-round record of surface ozone at coastal (Dumont d'Urville) and inland (Concordia) stations in East Antarctica, Journal of Geophysical Research: Atmospheres, 114(D20), https://doi.org/10.1029/2008JD011667, 2009.

Lei B., Min L.: Discussion on Maintenance of O_342M type Automatic Ozone Analyzer, Environmental Science Survey, 2014.

Legrand, M., Preunkert, S., Savarino, J., Frey, M.M., Kukui, A., Helmig, D., Jourdain, B., Jones, A.E., Weller, R., Brough, N., Gallée, H.: Inter-annual variability of surface ozone at coastal (Dumont d'Urville, 2004–2014) and inland (Concordia, 2007–2014) sites in East Antarctica, Atmos. Chem. Phys. 16, 8053–8069. http://dx. doi.org/10.5194/acp-16-8053-2016, 2016.

Liang, F., Cunde, X., Lingen, B.: Vertical Structure of Atmosphere on East Antarctic Plateau, Plateau Meteorology, 2015.

Lin, C., Gillespie, J., Schuder, M. D., Duberstein, W., Beverland, I. J., Heal, M. R.: Evaluation and calibration of aeroqual series 500 portable gas sensors for accurate measurement of ambient ozone and nitrogen dioxide, Atmospheric Environment, 100, 111-116, http://dx. doi.org/10.1016/j.atmosenv.2014.11.002, 2015.

Lin, M., Horowitz, L. W., Payton, R., Fiore, A. M., and Tonnesen, G.: US surface ozone trends and extremes from 1980 to 2014: quantifying the roles of rising Asian emissions, domestic controls, wildfires, and climate, Atmos. Chem. Phys., 17, 2943– 2970, https://doi.org/10.5194/acp-17-2943-2017, 2017.

Liu, J., Zhang, X. L., Zhang, X. C., Tang, J.: Surface Ozone Characteristics and the Correlated Factors at Shangdianzi Atmospheric Background Monitoring Station, Research of Environmental ences, https://doi.org/10.1016/S1872-2040(06)60041-8 , 2006.

Mickley, L. J., Murti, P. P., Jacob, D. J., Logan, J. A., Koch, D. M., and Rind, D.: Radiative forcing from tropospheric ozone calculated with a unified chemistry - climate model, Journal of Geophysical Research: Atmospheres, 104(D23), 30153-30172, https://doi.org/10.1029/1999JD900439, 1999.

Mihalikova, M., Kirkwood, S.: Tropopause fold occurrence rates over the Antarctic station Troll (72°S, 2.5°E), Ann. Geophys. 31, 591–598. http://dx.doi.org/10.5194/angeo-31-591-2013, 2013.

Monks, P. S., Archibald, A. T., Colette, A., Cooper, O., Coyle, M., Derwent, R., Fowler, D., Granier, C., Law, K. S., Mills, G. E., Stevenson, D. S., Tarasova, O., Thouret, V., von Schneidemesser, E., Sommariva, R., Wild, O., and Williams, M. L.: Tropospheric ozone and its precursors from the urban to the global scale from air quality to short-lived climate forcer, Atmos. Chem. Phys., 15, 8889–8973, https://doi.org/10.5194/acp-15-8889-2015, 2015.

Moura, Bárbara Bâesso, Souza, Sílvia Ribeiro de, Alves E S: Respostas estruturais em Ipomoea nil (L.) Roth 'Scarlet O'Hara' (Convolvulaceae) exposta ao ozônio, Acta Botanica Brasilica, 25(1):122-129, https://doi.org/10.1590/S0102-33062011000100015, 2011.

Murayama, S., Nakazawa, T., Tanaka, M., Aoki, S., Kawaguchi, S.: Variations of tropospheric ozone concentration over Syowa Station, Antarctica, Tellus B 44, 262–272, http://dx.doi.org/10.1034/j.1600-0889.1992.t01-3-00004.x, 1992.

Nadzir M S M , Ashfold M J , Khan M F , et al.: Spatial-temporal variations in surface ozone over Ushuaia and the Antarctic region: observations from in situ measurements, satellite data, and global models, Environmental ence & Pollution Research, http://dx.doi.org/10.1007/s11356-017-0521-1, 2018.

Neff, W., Helmig, D., Grachev, A., Davis, D.: A study of boundary layer behavior associated with high no concentrations at the south pole using a minisodar, tethered balloon, and sonic anemometer, Atmospheric Environment, 42(12), 2762-2779, http://dx.doi.org/10.1016/j.atmosenv.2007.01.033, 2008a.

Neff, W., Perlwitz, J., Hoerling, M.: Observational evidence for asymmetric changes in tropospheric heights over antarctica on decadal time scales, Geophysical Research Letters, 35(18), 102-102, http://dx.doi.org/10.1029/2008GL035074, 2008b.

Oltmans, S. J Komhyr, W. D.: Surface ozone in Antarctica, Journal of Geophysical Research, v. 81, p. 5359-5364. http://dx.doi.org/10.1029/jc081i030p05359,1976.

Oltmans, S. J., Johnson, B. J., & Helmig, D.: Episodes of high surface-ozone amounts at south pole during summer and their impact on the long-term surface-ozone variation, Atmospheric Environment, 42(12), 2804-2816, https://doi.org/10.1016/j.atmosenv, 2007.01.020, 2008.

Polissar, A., Hopke, P., Paatero, P., Kaufmann, Y., Hall, D., Bodhaine, B., Dutton, E., and Harris, J.: The aerosol at Barrow, Alaska: long-term trends and source locations, Atmos. Environ., 33, 2441–2458, https://doi.org/10.1016/s1352-2310(98)00423-3, 1999.

Prados-Roman C, Gómez L, Puentedura O, et al. Ground-based observations of Halogen Oxides in the Antarctic Boundary Layer[C]//EGU General Assembly Conference Abstracts. 2017, 19: 11798.

Putero, D., Cristofanelli, P., Sprenger, M., Škerlak, B., Tositti, L., and Bonasoni, P.: STEFLUX, a tool for investigating stratospheric intrusions: application to two WMO/GAW global stations, Atmos. Chem. Phys., 16, 14203-14217, https://doi.org/10.5194/acp-16-14203-2016, 2016.

Robinson, E., Clark, D., Cronn, DR.: Stratospheric-tropospheric Ozone Exchange in Antarctica Caused By Mountain Waves, Journal of Geophysical Research Oceans, 88(C15): 10708-10720, https://doi.org/10.1029/JC088iC15p10708, 1983.

Roscoe H K.: Possible descent across the “Tropopause” in Antarctic winter, Advances in Space Research, 33(7):1048-1052, https://doi.org/10.1016/S0273-1177(03)00587-8, 2004.

Sagona J A., Weisel C P., Meng Q.: Accuracy and practicality of a portable ozone monitor for personal exposure estimates, Atmospheric Environment, 175(FEB.):120-126, https://doi.org/10.1016/j.atmosenv.2017.11.036, 2018.

Schnell, R. C., Liu, S. C., Oltmans, S. J., Stone, R. S., Hofmann, D. J., Dutton, E. G.: Decrease of summer tropospheric ozone concentrations in antarctica, Nature, 351(6329), 726-729, https://doi.org/~~https://~~10.1038/351726a0, 1991.

~~Wang, S J., Tian, B., Ding, M H., Zhang, D Q., Zhang,T., Sun, W J.: Usage and performance assessment of a novel O_3 analyzer-model 205, OPTICAL INSTRUMENTS, 039(002), 58-63, 88, https://doi.org/10.3969/j.issn.1005-5630.2017.02.011, 2017.~~

Škerlak, B., Sprenger, M., and Wernli, H.: A global climatology of stratosphere–troposphere exchange using the ERA-Interim data set from 1979 to 2011, Atmos. Chem. Phys., 14, 913-937, https://doi.org/10.5194/acp-14-913-2014, 2014.

Slusher, D. L., Neff, W. D., Kim, S., Huey, L. G., Wang, Y., Zeng, T., Tanner, D. J., Blake, D. R., Beyersdorf, A., Lefer, B. L., Crawford, J. H., Eisele, F. L., Mauldin, R. L., Kosciuch, E., Buhr, M. P., Wallace, H. W., and Davis, D. D.:

Atmospheric chemistry results from the ANTCI 2005 Antarctic plateau airborne study. Journal of Geophysical Research: Atmospheres, Atmospheres, 115(D7), https://doi.org/10.1029/2009JD012605, 2010.

Sprovieri, F., Pirrone, N., Gaerdfeldt, K., Sommar, J.: Mercury speciation in the marine boundary layer along a 6000 km cruise path around the Mediterranean Sea, Atmospheric Environment, 37(1):63-71, https://doi.org/10.1016/S1352-2310(03)00237-1, 2003.

Stevenson, D. S., Johnson, C. E., Collins, W. J., Derwent, R. G., Shine, K. P., and Edwards, J. M.: Evolution of tropospheric ozone radiative forcing, Geophysical Research Letters, 25(20), 3819-3822, https://doi.org/10.1029/1998GL900037, 1998.

Stohl, A., Sodemann, H.: Characteristics of atmospheric transport into the Antarctic troposphere, J. Geophys. Res.: Atmosphere 115, D02305. http://dx.doi.org/10.1029/2009JD012536, 2010.

Traversi, R., Udisti, R., Frosini, D., Becagli, S., Ciardini, V., Funke, B., Lanconelli, C., Petkov, B., Scarchilli, C., Severi, M., Vitale, V.: Insights on nitrate sources at Dome C (East Antarctic Plateau) from multi-year aerosol and snow records, Tellus, B66, 22550, https://doi.org/10.3402/tellusb.v66.22550, 2014.

Traversi, R., Becagli, S., Brogioni, M., Caiazzo, L., Ciardini, V., Giardi, F., Legrand, M., Macelloni, G., Petkov, B., Preunkert, S., Scarchilli, C., Severi, M., Vitale, V., Udisti, R.: Multi-year record of atmospheric and snow surface nitrate in the central Antarctic plateau. Chemosphere 172, 341–354, http://www.sciencedirect.com/science/article/pii/S0045653516318872, 2017.

Wakamatsu, S., Ohara, T., and Uno, I.: Recent trends in precursor concentrations and oxidant distributions in the Tokyo and Osaka areas, Atmospheric Environment, 30(5), 715-721, https://doi.org/10.1016/1352-2310(95)00274-X, 1996.

Wang, S J., Tian, B., Ding, M H., Zhang, D Q., Zhang,T., Sun, W J.: Usage and performance assessment of a novel O_3 analyzer-model 205, OPTICAL INSTRUMENTS, 039(002), 58-63, 88, https://doi.org/10.3969/j.issn.1005-5630.2017.02.011, 2017.

Wang Y T., Bian L G., Ma Y F., Tang J., Zhang D Q., Zheng X D.: Surface ozone monitoring and background characteristics at Zhongshan Station over Antarctica. Chinese Sci Bull, 56(11), 848-857., https://doi.org/10.1007/s11434-011-4406-2, 2011.

Wang, Y. Q.: MeteoInfo: GIS software for meteorological data visualization and analysis, Meteorological Applications, 21(2), 360-368, https://doi.org/10.1002/met.1345, 2014.

Wong, JAHA.: Algorithm AS 136: A K-Means Clustering Algorithm, Journal of the Royal Statistical Society, 28:100-108, https://doi.org/10.2307/2346830, 1979.

Xu, W., Xu, X., Lin, M., Lin, W., Tarasick, D., Tang, J., Ma, J., and Zheng, X.: Long-term trends of surface ozone and its influencing factors at the Mt Waliguan GAW station, China – Part 2: The roles of anthropogenic emissions and climate variability, Atmos. Chem. Phys., 18, 773–798, https://doi.org/10.5194/acp-18-773-2018, 2018.

Ye, L., Bian, L., Tang, J., Ding, M., Zheng, X., Gao, Z.: A study on surface ozone depletion episodes over the A ntarctic coast, Acta Meteorologica Sinica, 75(3)，506-516, https://doi.org/ 10.11676/qxxb2017.027, 2017.

Yin, X., Kang, S., de Foy, B., Cong, Z., Luo, J., Zhang, L., Ma, Y., Zhang, G., Rupakheti, D., and Zhang, Q.: Surface ozone at Nam Co in the inland Tibetan Plateau: variation, synthesis comparison and regional representativeness, Atmos. Chem. Phys., 17, 11293-11311, https://doi.org/10.5194/acp-17-11293-2017, 2017.

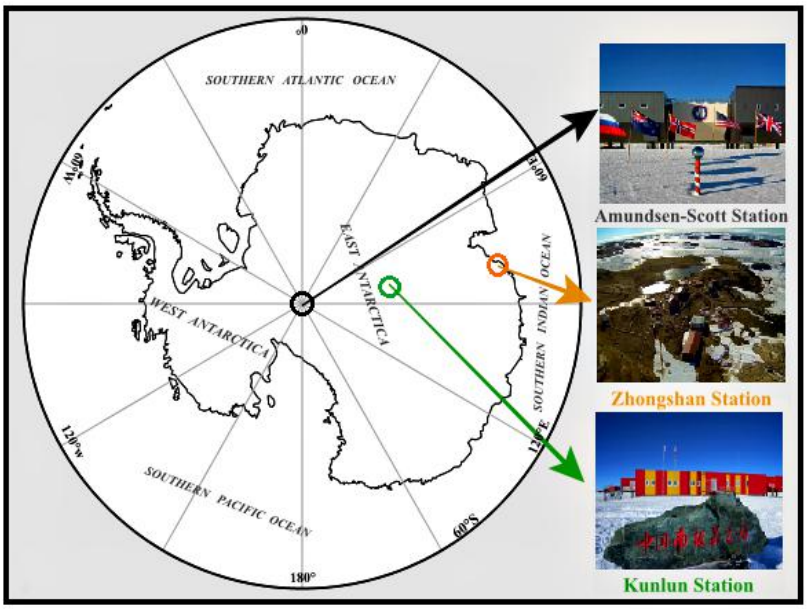

Figure 1: Amundsen-Scott Station (South Pole, SP), Kunlun Station (Dome A, DA) and Zhongshan Station (ZS) locations in Antarctica.

~~**Table 1. The specifications of Model 205**~~

~~**Instrument performance**~~	~~**Model 205**~~
~~Measuring Range~~	~~0ppb-100ppm~~

Weight (lb)	4.7 lb
Working flow (l)	> 1.2 l
Data storage (lines)	14336
Working temperature (°C)	0-50
Indication error (ppb / d)	< 1 ppb/d
Response time (s)	4
Signal interface	RS232

710 **Table.1 Comparison of the working parameters in the three instruments**

Instrument performance	Model 205	Ecotech 9810A	Thermo 49C
Measuring Range	0ppb-100ppm	0ppb-20ppm	0ppb-200ppm
Weight (kg)	2.2kg	21	15.9
Working flow (L/min)	> 1.2	$0.5*10^{-3}$	1~3
Data storage (lines)	14336	50400	115200
Working temperature (℃)	0-50	5-40	0-45
Indication error (ppb / d)	< 1 ppb/d	< 1 ppb/d	< 1 ppb/d
Response time (s)	4	60	20
Signal interface	RS232	RS232, USB	RS232, RS485,RJ45

Table 212. The calibration record of ozone monitor

Date	Span Point (ppb)	Thermo 49ips (ppb)	Model 205 (ppb)
2015/10/5	0	0.79	0.26
	20	19.99	20.73
	35	34.99	35.35
	50	50.02	50.73
	65	64.96	65.71

	~~80~~	~~79.99~~	~~80.48~~
	~~100~~	~~99.99~~	~~100.43~~
	~~120~~	~~119.96~~	~~120.31~~
~~2017/5/6~~	~~0~~	~~-0.71~~	~~0.51~~
	~~20~~	~~20.00~~	~~21.68~~
	~~35~~	~~34.95~~	~~36.95~~
	~~50~~	~~50.01~~	~~52.17~~
	~~65~~	~~64.98~~	~~67.37~~
	~~80~~	~~79.99~~	~~82.88~~
	~~100~~	~~100.00~~	~~103.00~~
	~~120~~	~~119.92~~	~~124.10~~

715 **Table 1. The calibration record of ozone monitor**

Date	Span Point （ppb）	Thermo 49ips （ppb）	Model 205 （ppb）
2015/10/5	0	-0.79	0.26
	20	19.99	20.73
	35	34.99	35.35
	50	50.02	50.73
	65	64.96	65.71
	80	79.99	80.48
	100	99.99	100.43
	120	119.96	120.31
2017/5/6	0	-0.71	0.51
	20	20.00	21.68
	35	34.95	36.95
	50	50.01	52.17
	65	64.98	67.37
	80	79.99	82.88
	100	100.00	103.00
	120	119.92	124.10

720

Table ~~3~~2. Stability test of ozone monitor.

Time	Slope	Standard Uncertainty	Intercept	Standard Uncertainty
2015/10/5	0.99936	0.00195	0.53861	0.13672
2017/5/6	1.02520	0.00264	0.85220	0.18491
Average	1.01228	0.00230	0.69541	0.16082
Standard Error	0.01827	0.00049	0.22174	0.03408

725

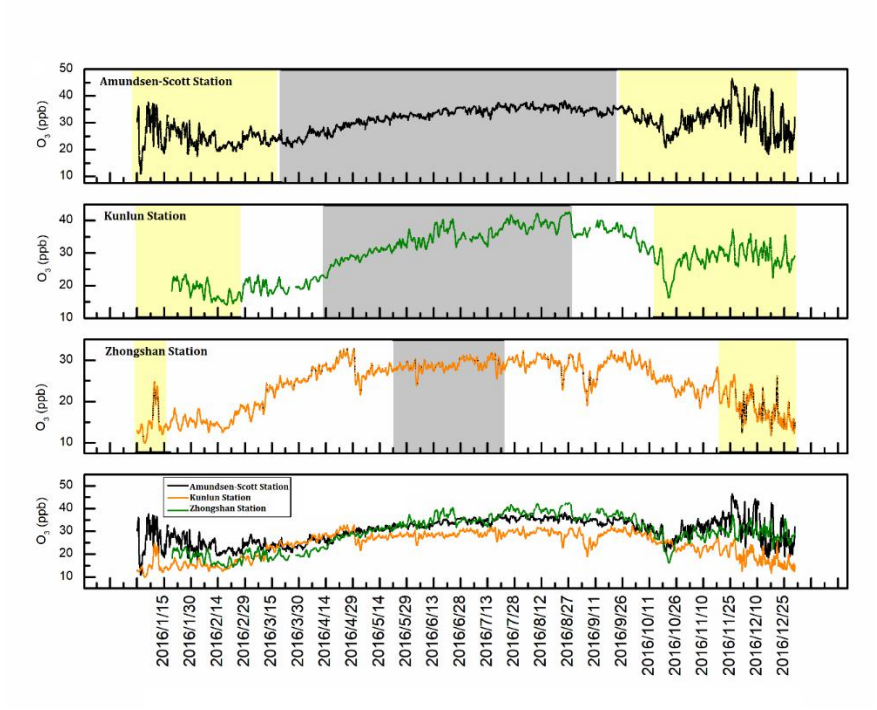
Amundsen-Scott Station
Kunlun Station
Zhongshan Station
Amundsen-Scott Station
Kunlun Station
Zhongshan Station
O3 (ppb)
2016/1/15
2016/1/30
2016/2/14
2016/2/29
2016/3/15
2016/3/30
2016/4/14
2016/4/29
2016/5/14
2016/5/29
2016/6/13
2016/6/28
2016/7/13
2016/7/28
2016/8/12
2016/8/27
2016/9/11
2016/9/26
2016/10/11
2016/10/26
2016/11/10
2016/11/25
2016/12/10
2016/12/25

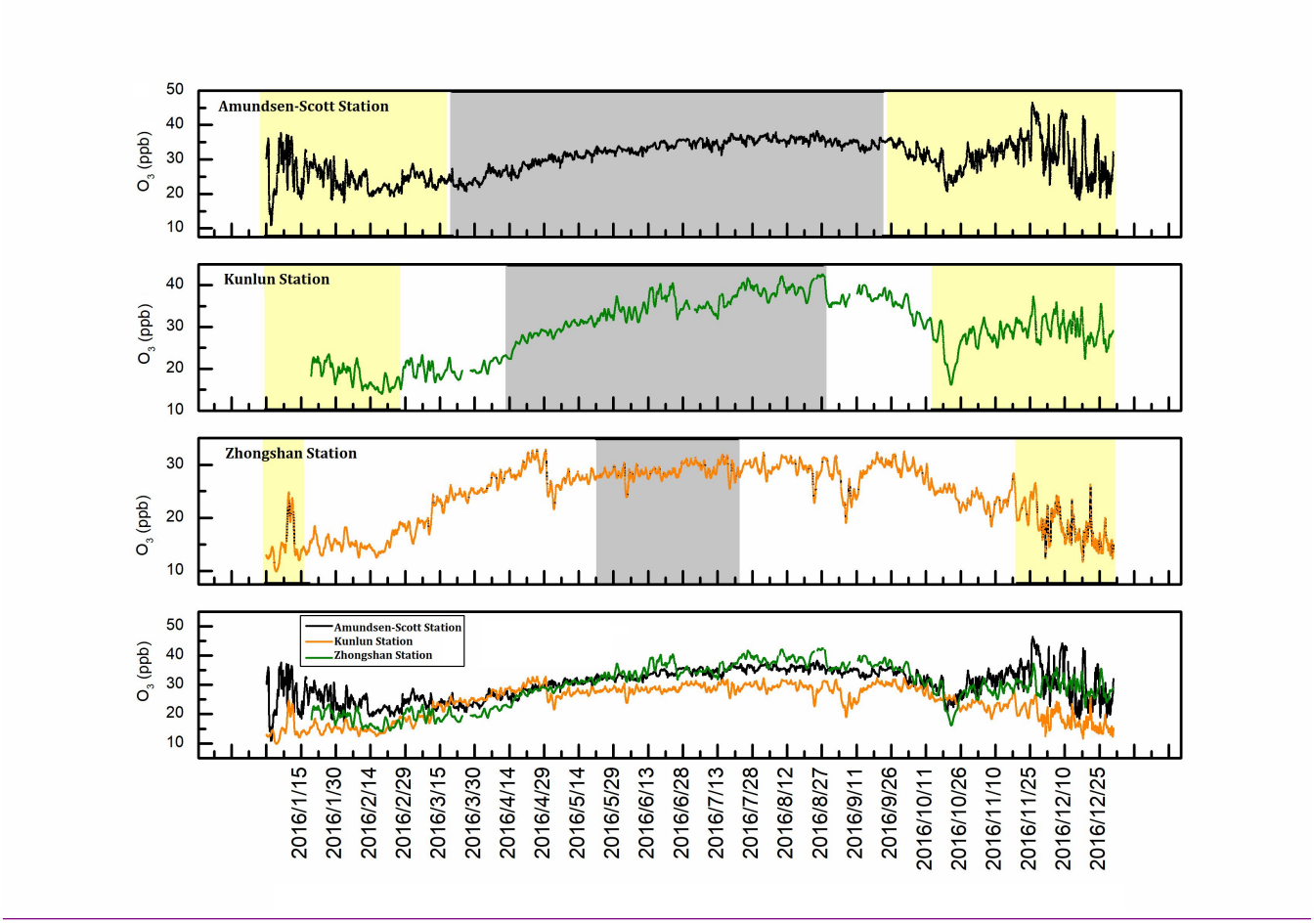

Figure 2: Time series of near-surface O_3 at the SP, DA and ZS during 2016. Yellow (grey) shading identifies polar day (night).

730

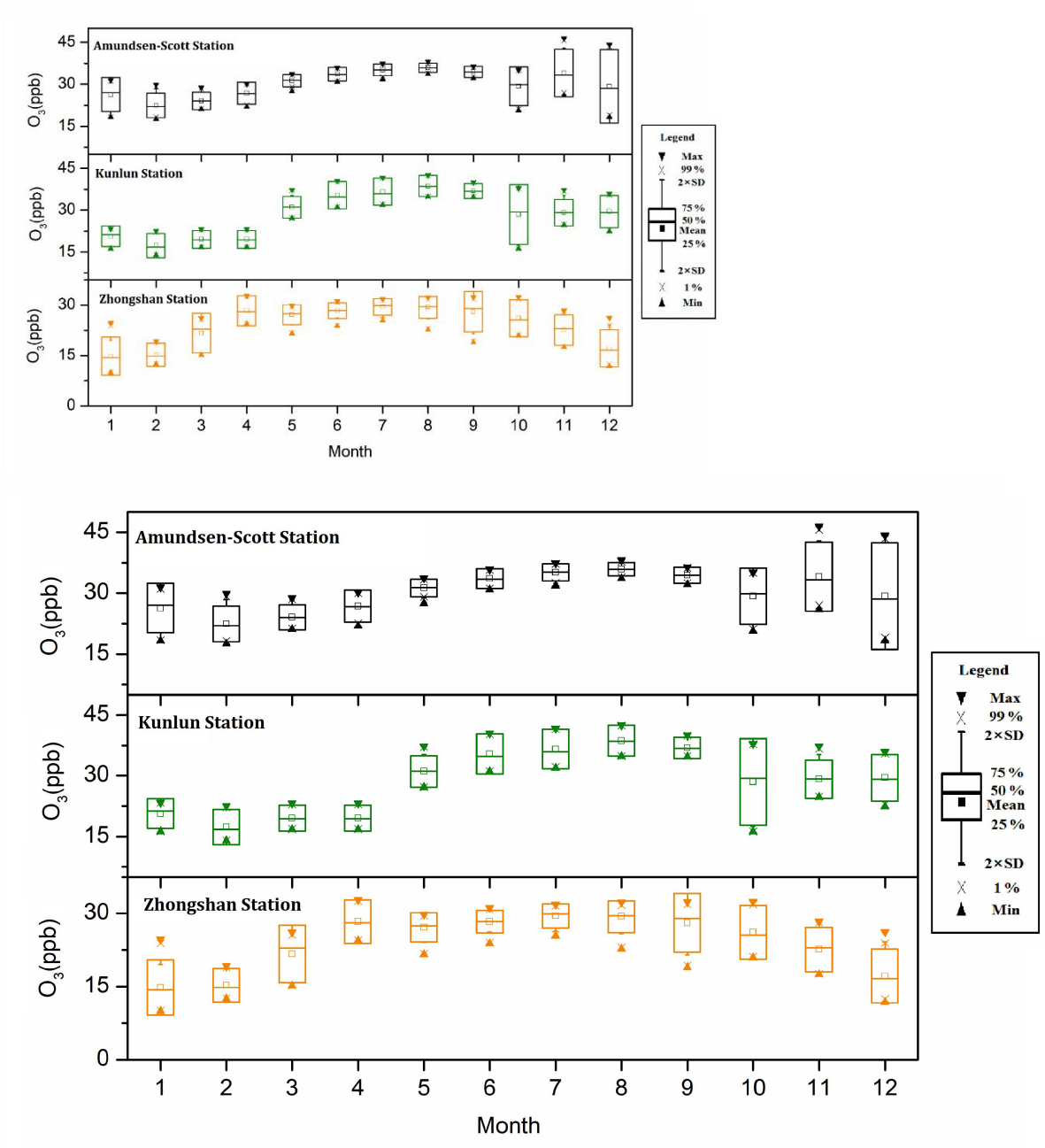

Figure 3: Monthly average and statistical parameters of near-surface O_3 at the SP, DA and ZS during 2016.

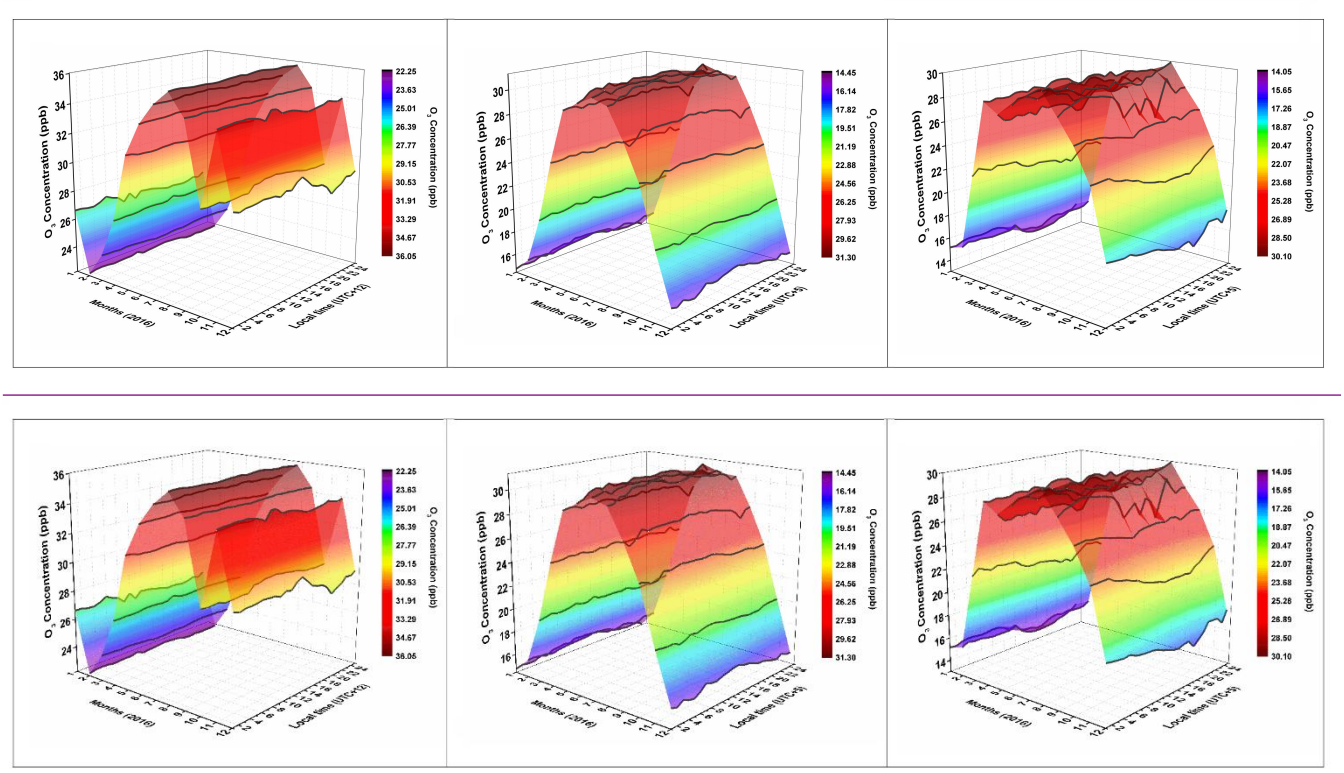

735

Figure 4: Mean diurnal variations in near-surface O_3 concentrations at the SP (a), DA (b) and ZS (c) during 2016.

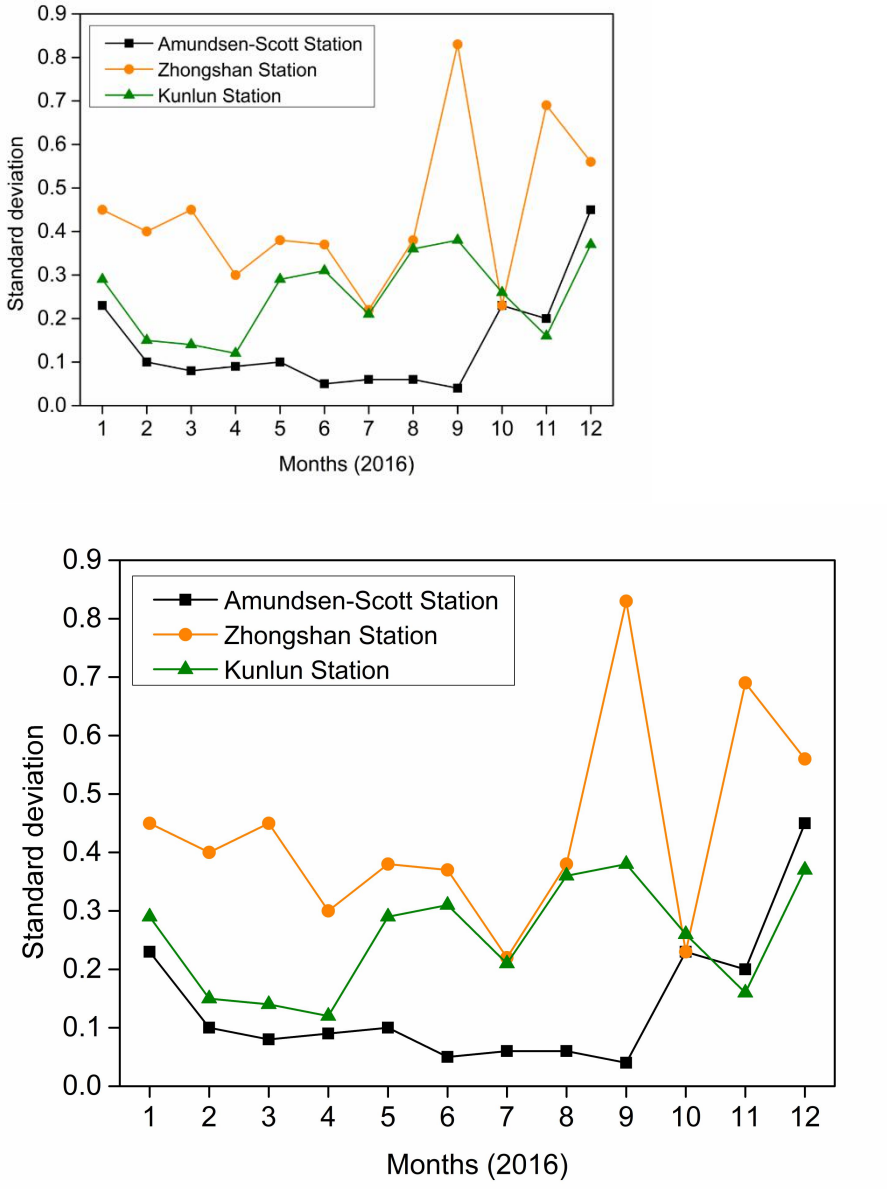

Figure 5: Standard deviations of mean diurnal variation in near-surface~~Standard deviation of mean diurnal variations in near-surface~~ O_3 **concentrations at the SP, DA and ZS during 2016.**

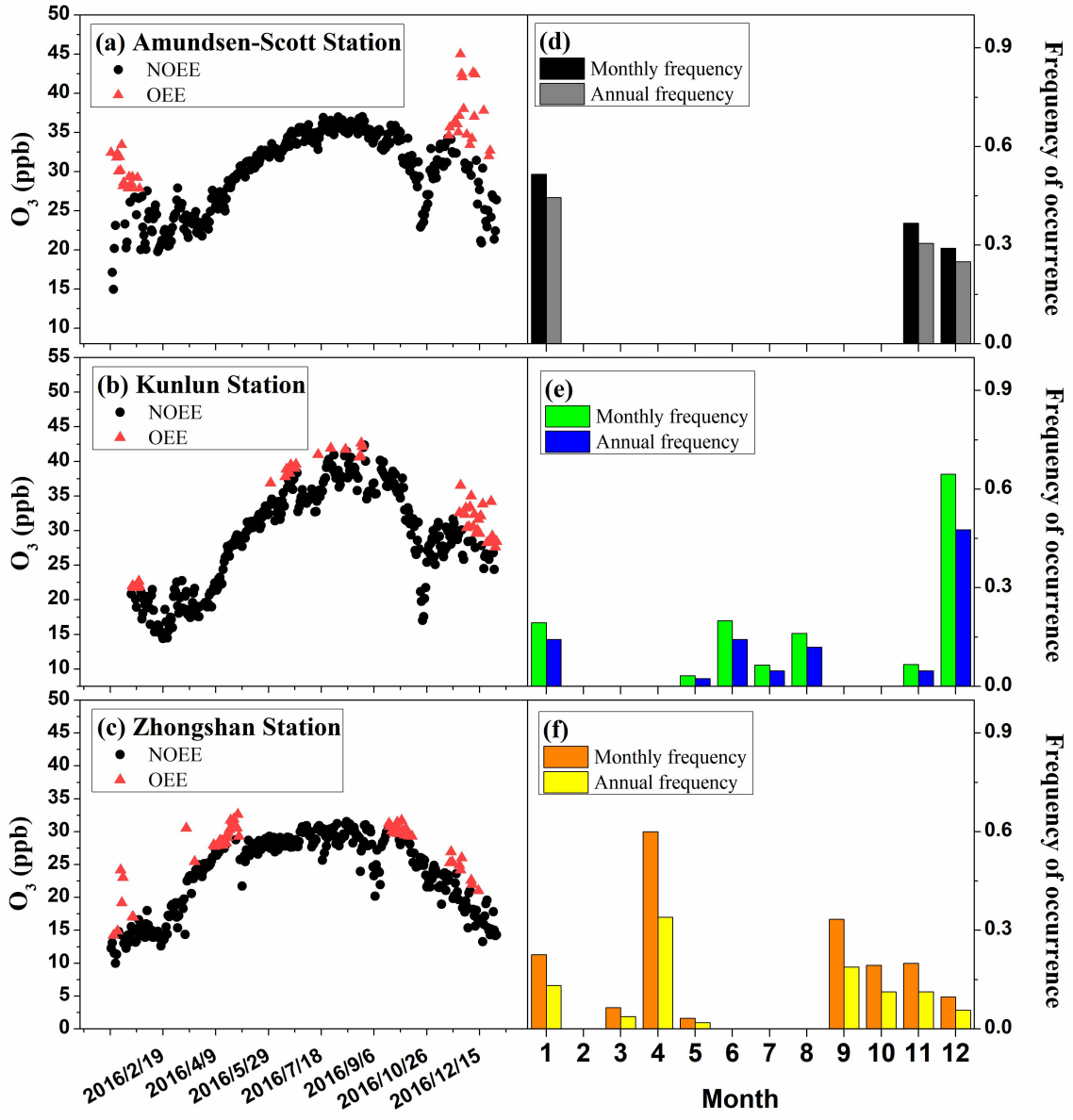
(a) Amundsen-Scott Station
NOEE
OEE
(b) Kunlun Station
NOEE
OEE
(c) Zhongshan Station
NOEE
OEE
(d)
Monthly frequency
Annual frequency
(e)
Monthly frequency
Annual frequency
(f)
Monthly frequency
Annual frequency
O3 (ppb)
Frequency of occurrence
2016/2/19
2016/4/9
2016/5/29
2016/7/18
2016/9/6
2016/10/26
2016/12/15
1 2 3 4 5 6 7 8 9 10 11 12
Month

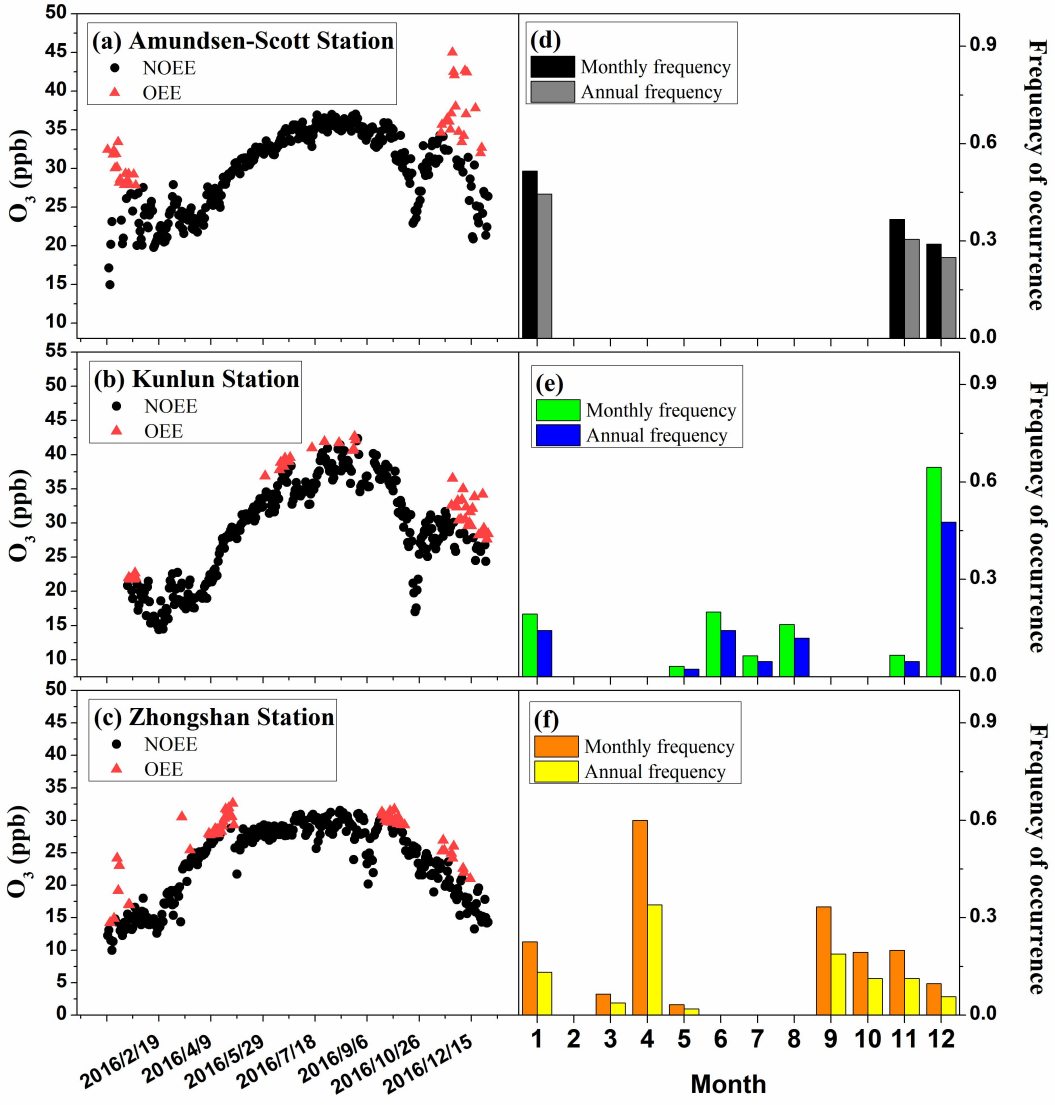
(a) Amundsen-Scott Station
NOEE
OEE
(b) Kunlun Station
NOEE
OEE
(c) Zhongshan Station
NOEE
OEE
(d)
Monthly frequency
Annual frequency
(e)
Monthly frequency
Annual frequency
(f)
Monthly frequency
Annual frequency
O3 (ppb)
Frequency of occurrence
2016/2/19
2016/4/9
2016/5/29
2016/7/18
2016/9/6
2016/10/26
2016/12/15
1 2 3 4 5 6 7 8 9 10 11 12
Month

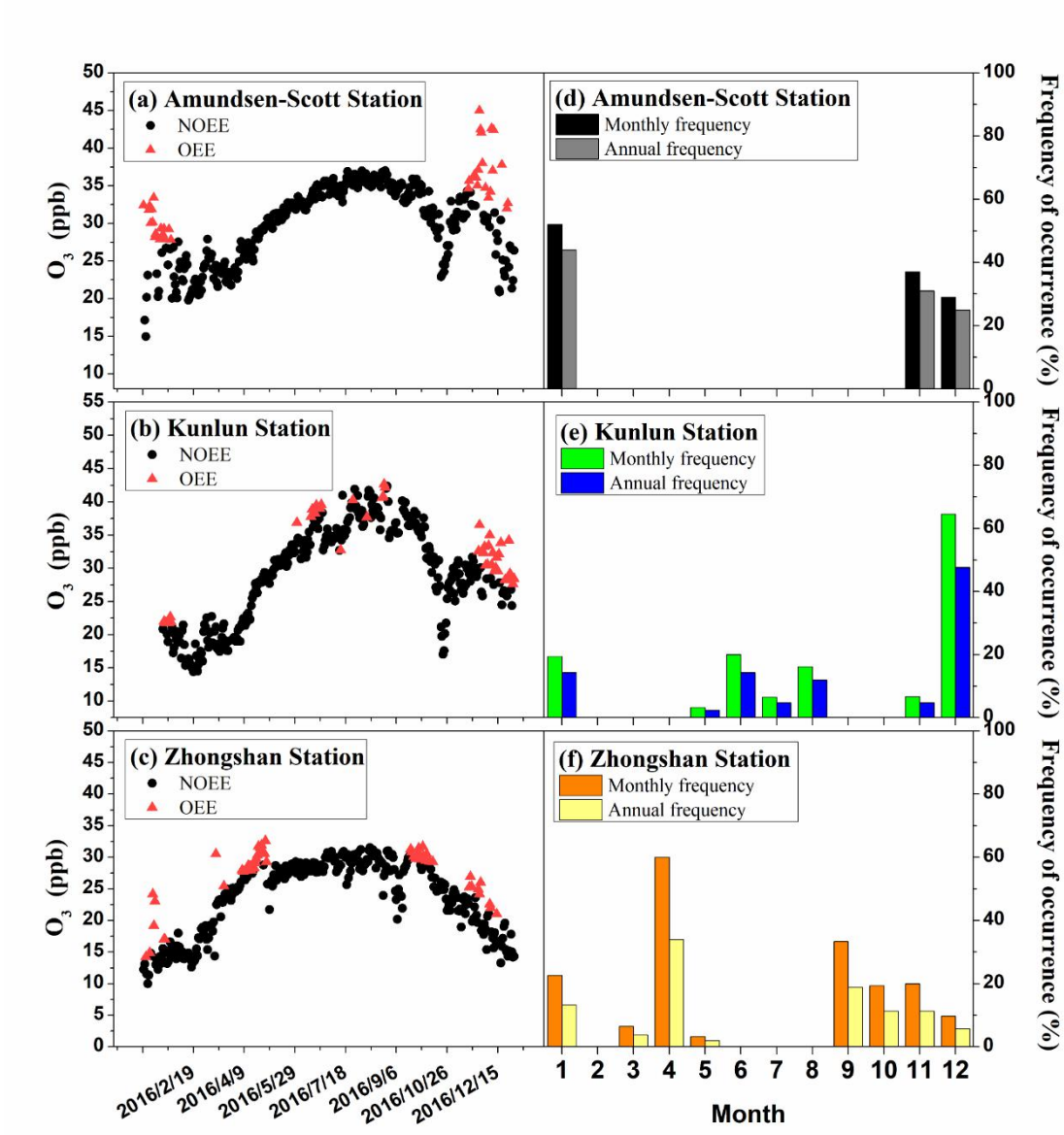

Figure 6: (a, b and c) The OEEs and (d, e and f) averaged distribution of OEE occurrence among the different months of 2016 at the three stations. $\boldsymbol{Monthly\ frequency} = \frac{\text{number of OEE days for each month}}{\text{number of days in the month}}$; $\boldsymbol{Annual\ frequency} = \frac{\text{number of OEE days for each month}}{\text{total number of OEE days}}$.

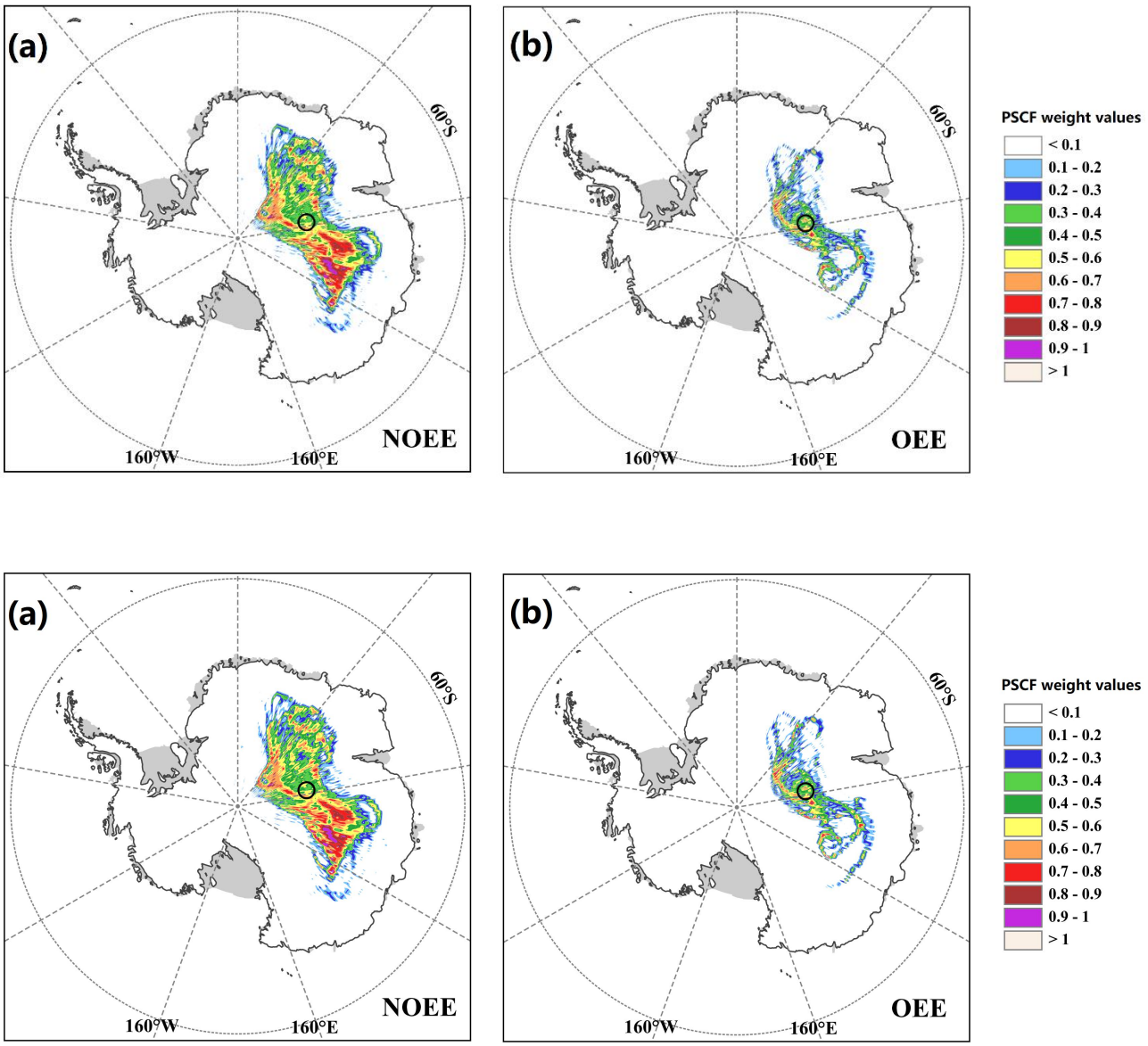

Figure 7: Likely source areas of surface O_3 at Kunlun Station during the NOEE (a) and OEE (b) identified using the PSCF (Potential Source Contribution Function).

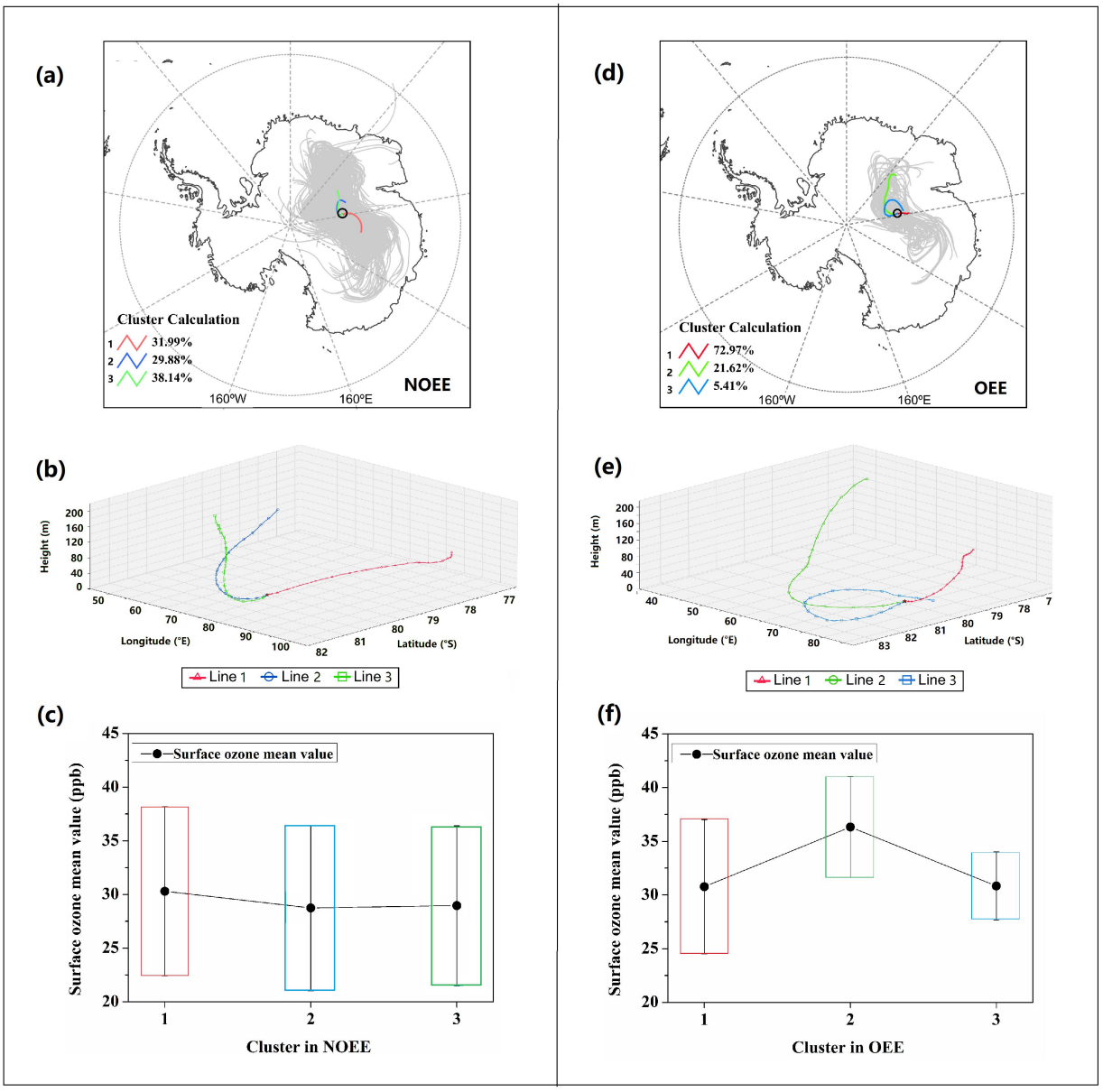
(a)
Cluster Calculation
1 31.99%
2 29.88%
3 38.14%
160°W
160°E
NOEE
(d)
Cluster Calculation
1 72.97%
2 21.62%
3 5.41%
160°W
160°E
OEE
(b)
Height (m)
Longitude (°E)
Latitude (°S)
Line 1
Line 2
Line 3
(e)
Height (m)
Longitude (°E)
Latitude (°S)
Line 1
Line 2
Line 3
(c)
Surface ozone mean value
Surface ozone mean value (ppb)
Cluster in NOEE
(f)
Surface ozone mean value
Surface ozone mean value (ppb)
Cluster in OEE

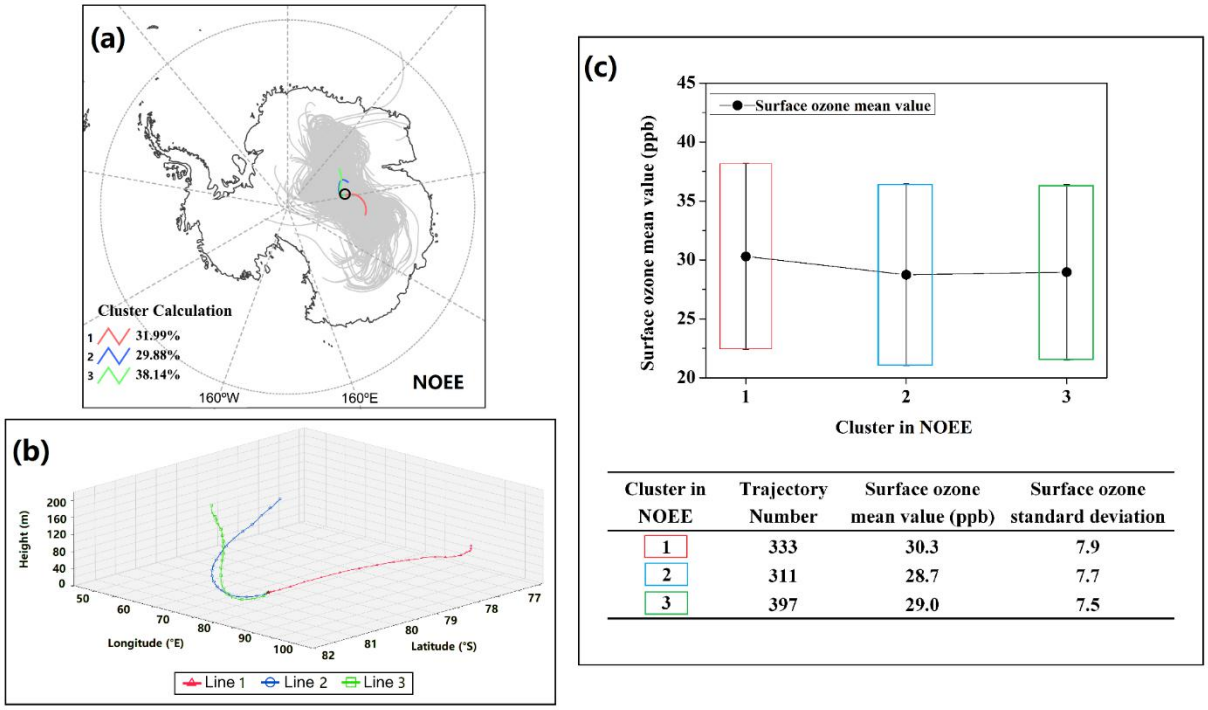

Cluster in NOEE	Trajectory Number	Surface ozone mean value (ppb)	Surface ozone standard deviation
1	333	30.3	7.9
2	311	28.7	7.7
3	397	29.0	7.5

Figure 8: Backward HYSPLIT trajectories for each measurement day (gray lines in ~~Fig.~~Figure 8a), and mean back trajectory for 3 HYSPLIT clusters (colored lines in ~~Fig.~~Figure 8a, 3D view shown in ~~Fig.~~Figure 8b) arriving at Kunlun Station during NOEEs. Subplot (c) shows the range of surface ozone ~~mixing ratio~~concentrations measured at ~~Kunlun Station~~DA by cluster. Error bars is~~are~~ the standard deviation of the same cluster. Same as subplot (a, b, c), but subplot (d, e, f) for OEEs.

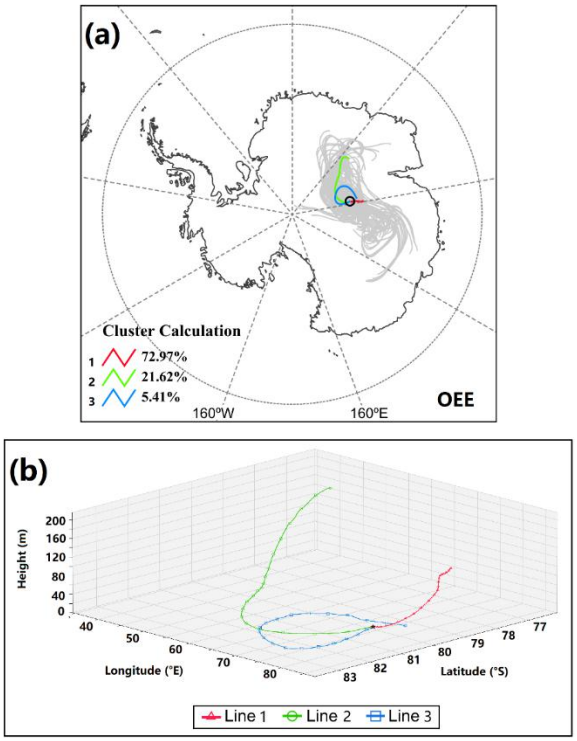

Cluster in OEE	Trajectory Number	Surface ozone mean value (ppb)	Surface ozone standard deviation
1	108	30.8	6.3
2	32	36.3	4.7
3	8	30.8	3.2

~~Figure 9: Same as Fig.~~Figure 8~~, but for OEEs.~~

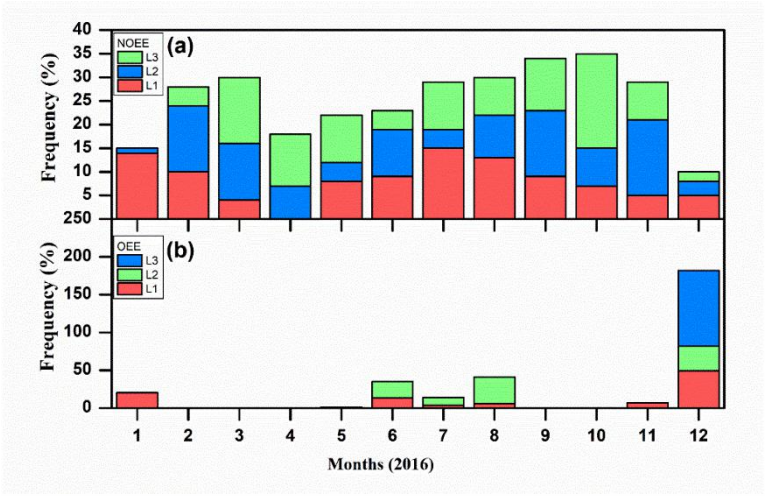

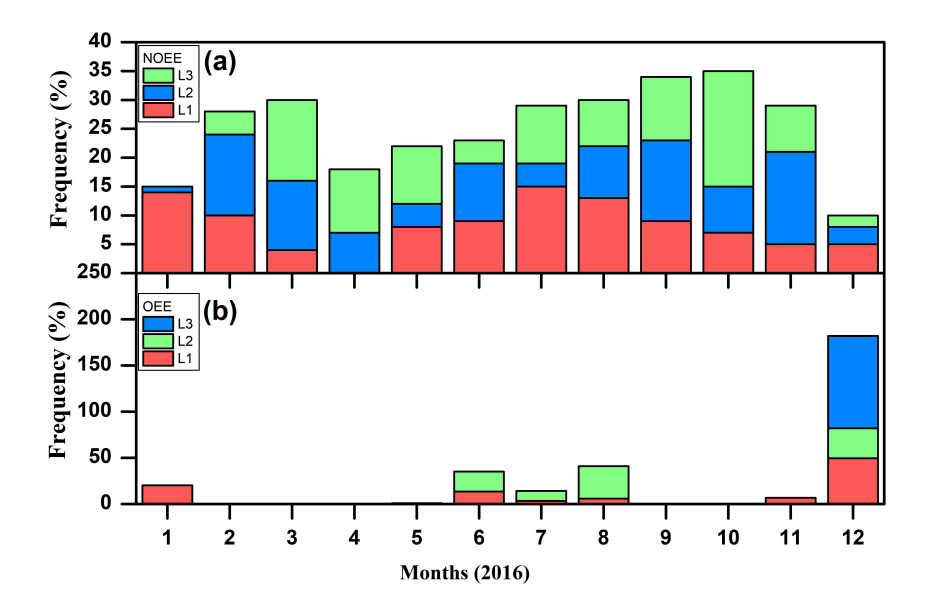

765

Figure ~~10~~9: Monthly frequency distribution of clustering trajectories (Line 1, 2, 3) during NOEEs and OEEs.

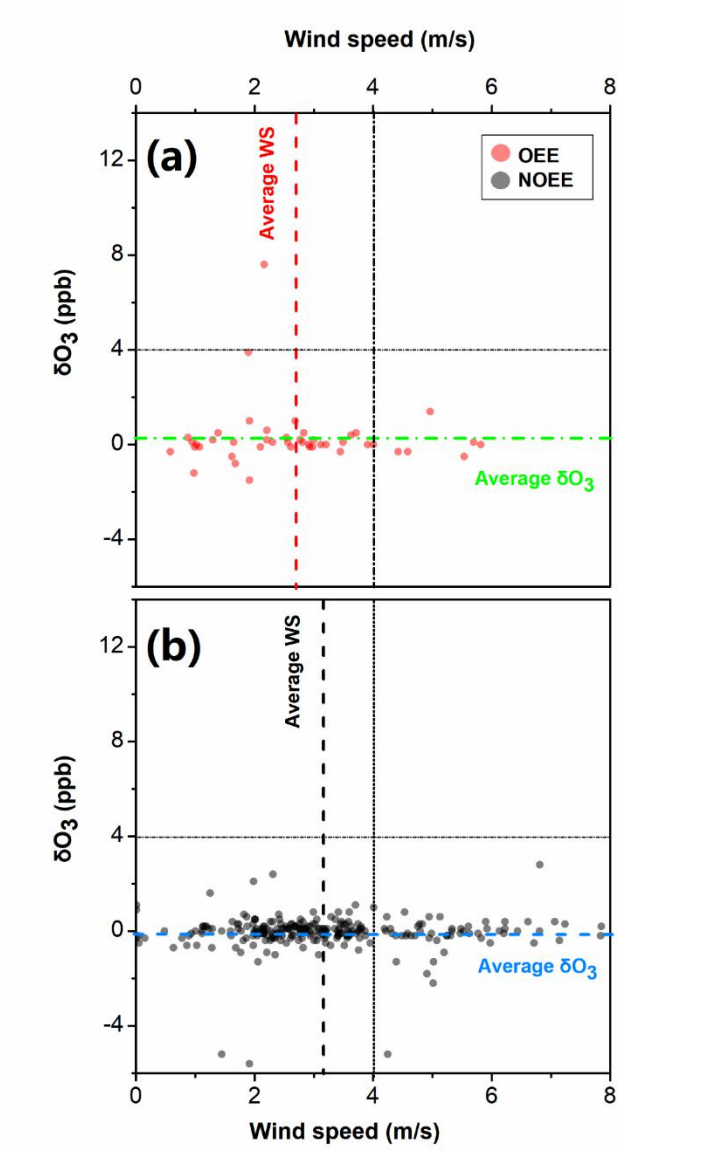
Wind speed (m/s)
(a)
Average WS
OEE
NOEE
Average δO3
δO3 (ppb)
(b)
Average WS
Average δO3
δO3 (ppb)
Wind speed (m/s)

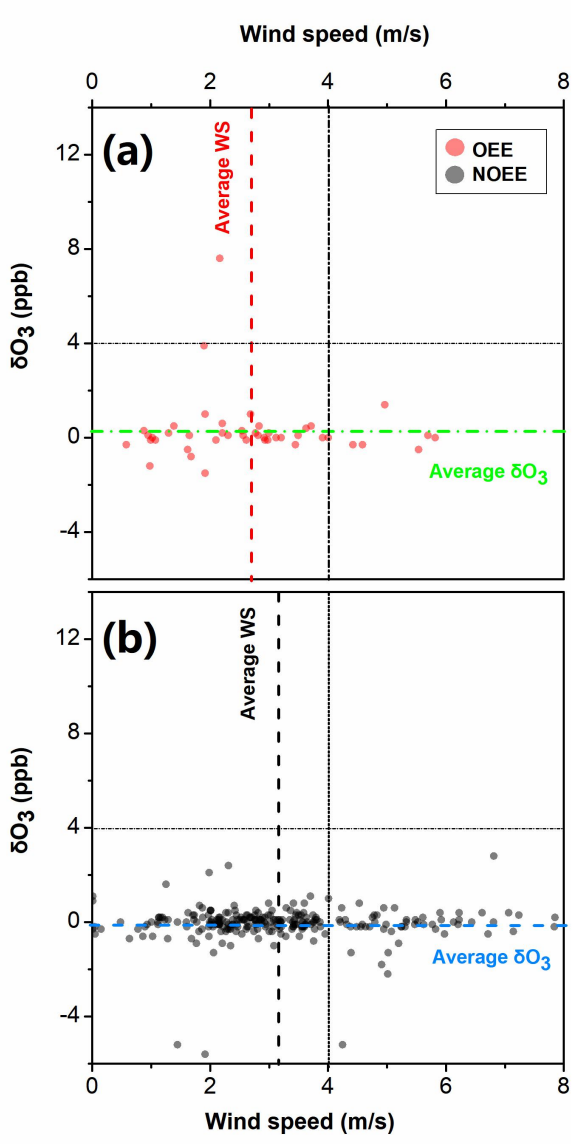

Figure ~~11~~10: Wind speed and ~~δ~~ΔO3 ~~O3~~ statistical distribution around OEEs (red dots) and NOEEs (black dots) at DA in polar night. Here, ΔO3~~δO3~~ represents the growth rate of near-surface O3 concentration, calculated by equation:

$$\Delta O3\delta O_3 = \frac{\text{The O3 concentration at } T_n - \text{ The O3 concentration at } T_{n-1}}{\text{Time difference of } T_n \text{ and } T_{n-1}}$$

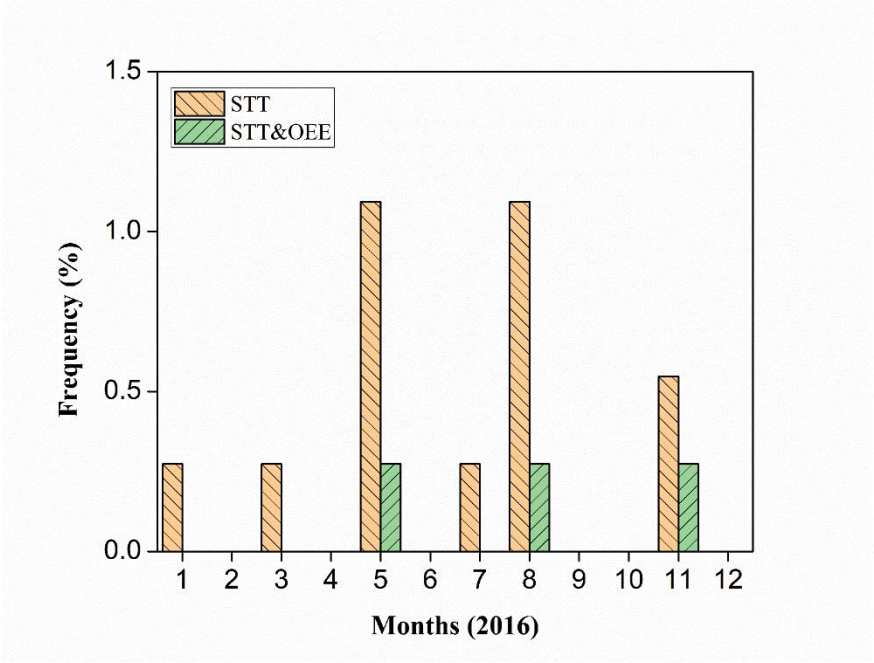
STT
STT&OEE
Frequency (%)
1.5
1.0
0.5
0.0
1 2 3 4 5 6 7 8 9 10 11 12
Months (2016)

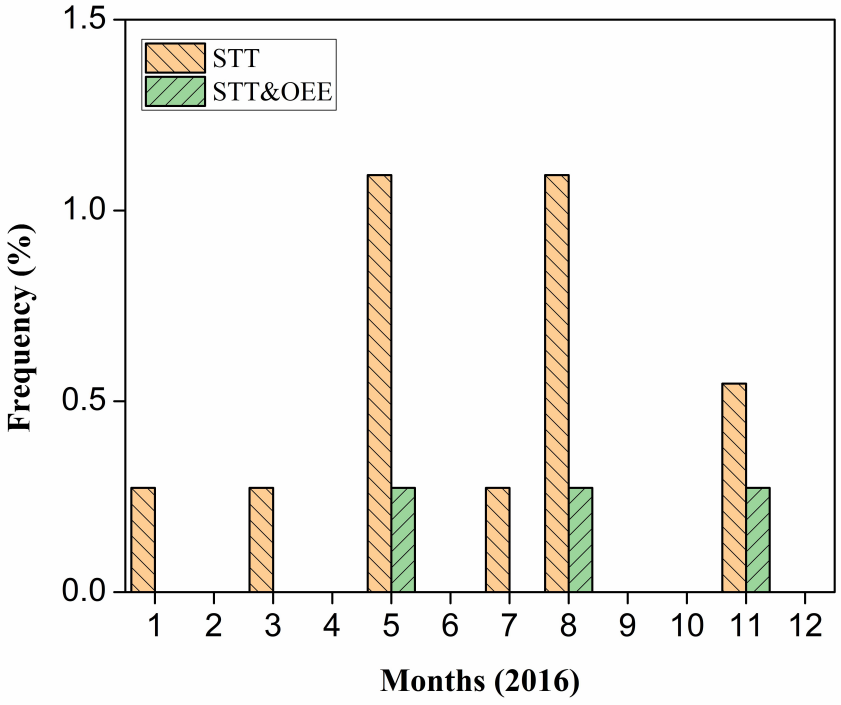
STT
STT&OEE
Frequency (%)
1.5
1.0
0.5
0.0
1 2 3 4 5 6 7 8 9 10 11 12
Months (2016)

Figure ~~12~~11: Annual variation of "deep" STT events at Kunlun Station and the annual variation of it occurred at the same time with OEE over the period 2016, obtained by STEFLUX.